ESCUELA TÉCNICA SUPERIOR DE INGENIERÍA (ICAI)

INGENIERO INDUSTRIAL

STRUCTURAL ANALYSIS OF THE IRRADIATION-INDUCED LONGITUDINAL GROWTH OF A PWR FUEL ASSEMBLY DURING NORMAL OPERATION USING THE FINITE ELEMENT METHOD

Autor: Isabel Cabrera Millán
Director: Prof. Dr. Rafael Macián-Juan

Madrid
Mayo 2015

Proyecto realizado por el alumno/a:

Isabel Cabrera Millán

Fdo.: ..... Fecha: 19 / 05 / 2015

Autorizada la entrega del proyecto cuya información no es de carácter confidencial

EL DIRECTOR DEL PROYECTO

Rafael Macián Juan

Fdo.: ..... Fecha: 19 / 05 / 2015

Vº Bº del Coordinador de Proyectos

(poner el nombre del Coordinador de Proyectos)

Fdo.: ..... Fecha: ..... / ..... / .....

AUTORIZACIÓN PARA LA DIGITALIZACIÓN, DEPÓSITO Y DIVULGACIÓN EN ACCESO *ABIERTO* (*RESTRINGIDO*) DE DOCUMENTACIÓN

1º. Declaración de la autoría y acreditación de la misma.

El autor D. _____ , como _____ de la UNIVERSIDAD PONTIFICIA COMILLAS (COMILLAS), **DECLARA**

que es el titular de los derechos de propiedad intelectual, objeto de la presente cesión, en relación con la obra_____ _____[1], que ésta es una obra original, y que ostenta la condición de autor en el sentido que otorga la Ley de Propiedad Intelectual como titular único o cotitular de la obra.

En caso de ser cotitular, el autor (firmante) declara asimismo que cuenta con el consentimiento de los restantes titulares para hacer la presente cesión. En caso de previa cesión a terceros de derechos de explotación de la obra, el autor declara que tiene la oportuna autorización de dichos titulares de derechos a los fines de esta cesión o bien que retiene la facultad de ceder estos derechos en la forma prevista en la presente cesión y así lo acredita.

2º. Objeto y fines de la cesión.

Con el fin de dar la máxima difusión a la obra citada a través del Repositorio institucional de la Universidad y hacer posible su utilización de *forma libre y gratuita* (*con las limitaciones que más adelante se detallan*) por todos los usuarios del repositorio y del portal e-ciencia, el autor **CEDE** a la Universidad Pontificia Comillas de forma gratuita y no exclusiva, por el máximo plazo legal y con ámbito universal, los derechos de digitalización, de archivo, de reproducción, de distribución, de comunicación pública, incluido el derecho de puesta a disposición electrónica, tal y como se describen en la Ley de Propiedad Intelectual. El derecho de transformación se cede a los únicos efectos de lo dispuesto en la letra (a) del apartado siguiente.

3º. Condiciones de la cesión.

[1] Especificar si es una tesis doctoral, proyecto fin de carrera, proyecto fin de Máster o cualquier otro trabajo que deba ser objeto de evaluación académica

Sin perjuicio de la titularidad de la obra, que sigue correspondiendo a su autor, la cesión de derechos contemplada en esta licencia, el repositorio institucional podrá:

(a) Transformarla para adaptarla a cualquier tecnología susceptible de incorporarla a internet; realizar adaptaciones para hacer posible la utilización de la obra en formatos electrónicos, así como incorporar metadatos para realizar el registro de la obra e incorporar "marcas de agua" o cualquier otro sistema de seguridad o de protección.

(b) Reproducirla en un soporte digital para su incorporación a una base de datos electrónica, incluyendo el derecho de reproducir y almacenar la obra en servidores, a los efectos de garantizar su seguridad, conservación y preservar el formato. .

(c) Comunicarla y ponerla a disposición del público a través de un archivo abierto institucional, accesible de modo libre y gratuito a través de internet.[2]

(d) Distribuir copias electrónicas de la obra a los usuarios en un soporte digital. [3]

4º. Derechos del autor.

El autor, en tanto que titular de una obra que cede con carácter no exclusivo a la Universidad por medio de su registro en el Repositorio Institucional tiene derecho a:

a) A que la Universidad identifique claramente su nombre como el autor o propietario de los derechos del documento.

b) Comunicar y dar publicidad a la obra en la versión que ceda y en otras posteriores a través de cualquier medio.

c) Solicitar la retirada de la obra del repositorio por causa justificada. A tal fin deberá ponerse en contacto con el vicerrector/a de investigación (curiarte@rec.upcomillas.es).

d) Autorizar expresamente a COMILLAS para, en su caso, realizar los trámites necesarios para la obtención del ISBN.

---

[2] En el supuesto de que el autor opte por el acceso restringido, este apartado quedaría redactado en los siguientes términos:

(c) Comunicarla y ponerla a disposición del público a través de un archivo institucional, accesible de modo restringido, en los términos previstos en el Reglamento del Repositorio Institucional

[3] En el supuesto de que el autor opte por el acceso restringido, este apartado quedaría eliminado.

d) Recibir notificación fehaciente de cualquier reclamación que puedan formular terceras personas en relación con la obra y, en particular, de reclamaciones relativas a los derechos de propiedad intelectual sobre ella.

5º. Deberes del autor.

El autor se compromete a:

a) Garantizar que el compromiso que adquiere mediante el presente escrito no infringe ningún derecho de terceros, ya sean de propiedad industrial, intelectual o cualquier otro.

b) Garantizar que el contenido de las obras no atenta contra los derechos al honor, a la intimidad y a la imagen de terceros.

c) Asumir toda reclamación o responsabilidad, incluyendo las indemnizaciones por daños, que pudieran ejercitarse contra la Universidad por terceros que vieran infringidos sus derechos e intereses a causa de la cesión.

d) Asumir la responsabilidad en el caso de que las instituciones fueran condenadas por infracción de derechos derivada de las obras objeto de la cesión.

6º. Fines y funcionamiento del Repositorio Institucional.

La obra se pondrá a disposición de los usuarios para que hagan de ella un uso justo y respetuoso con los derechos del autor, según lo permitido por la legislación aplicable, y con fines de estudio, investigación, o cualquier otro fin lícito. Con dicha finalidad, la Universidad asume los siguientes deberes y se reserva las siguientes facultades:

a) Deberes del repositorio Institucional:

- La Universidad informará a los usuarios del archivo sobre los usos permitidos, y no garantiza ni asume responsabilidad alguna por otras formas en que los usuarios hagan un uso posterior de las obras no conforme con la legislación vigente. El uso posterior, más allá de la copia privada, requerirá que se cite la fuente y se reconozca la autoría, que no se obtenga beneficio comercial, y que no se realicen obras derivadas.

- La Universidad no revisará el contenido de las obras, que en todo caso permanecerá bajo la responsabilidad exclusiva del autor y no estará obligada a ejercitar acciones legales en nombre del autor en el supuesto de infracciones a derechos de propiedad intelectual derivados del depósito y archivo de las obras. El autor renuncia a cualquier reclamación frente a la Universidad por las formas no ajustadas a la legislación vigente en que los usuarios hagan uso de las obras.

- La Universidad adoptará las medidas necesarias para la preservación de la obra en un futuro.

b) Derechos que se reserva el Repositorio institucional respecto de las obras en él registradas:

- retirar la obra, previa notificación al autor, en supuestos suficientemente justificados, o en caso de reclamaciones de terceros.

Madrid, a …….. de …….. de …….

ACEPTA

Fdo……

ANÁLISIS ESTRUCTURAL DEL CRECIMIENTO LONGITUDINAL DE UN ELEMENTO DE COMBUSTIBLE DE UN PWR BAJO IRRADIACIÓN USANDO EL MÉTODO DE ELEMENTOS FINITOS

Autor: Isabel Cabrera Millán

Director: Prof. Dr. Rafael Macián-Juan.

Entidad Colaboradora: TUM- Technische Universität München, Lehrstuhl für Nukleartechnik.

RESUMEN DEL PROYECTO

Introducción

Un reactor de agua a presión (PWR por sus siglas en inglés) es uno de los tipos de reactores nucleares más utilizados a nivel mundial. La principal característica de este tipo de reactores es la alta presión en el interior de la vasija del núcleo (alrededor de 15MPa) con el fin de evitar la ebullición del agua en su interior.

El arqueamiento de los elementos de combustible de los PWR es un campo activo de investigación hoy en día, puesto que puede provocar problemas tanto funcionales como de seguridad en el reactor. Sin embargo, la realización de pruebas experimentales teniendo en cuenta todas las condiciones de funcionamiento de un PWR que afectan a este fenómeno sería extremadamente complejo. Por este motivo, la creación de un modelo informático de un elemento de combustible de un PWR es necesaria para el estudio de su arqueamiento.

El objetivo de este proyecto es la realización de un análisis estructural del crecimiento axial de un elemento de combustible de un PWR bajo irradiación, como una parte del estudio del arqueamiento de la estructura. Dicho estudio se basa en un modelo ya existente de un elemento de combustible, implementado en ANSYS, que usa el método de elementos finitos.

Una estructura típica de estos elementos de combustible se muestra en la siguiente figura.

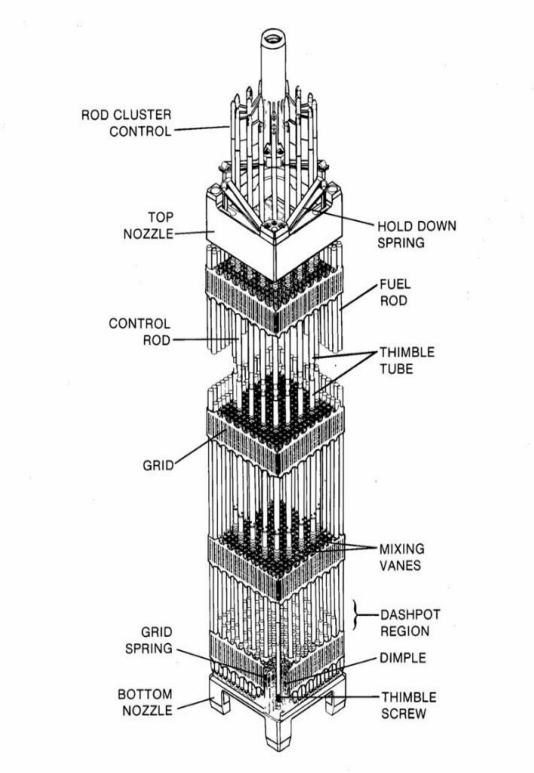

Ilustración 1 Elemento de combustible de un PWR

Metodología

Para la realización del análisis axial del elemento de combustible de un PWR, se han tenido en cuenta las siguientes fuerzas axiales que actúan en el núcleo del reactor a lo largo del ciclo de irradiación.

1) Fuerzas de flotación: los elementos de combustible, que se encuentran situados en el interior de la vasija del reactor, están sumergidos en agua, que funciona como refrigerante y moderador de neutrones. Por ello se crean las llamadas fuerzas de flotación.
   En este análisis, el valor de estas fuerzas han sido calculado, y han sido aplicadas como fuerzas puntuales en la base de cada elemento, en este caso de cada barra de combustible y de cada tubo guía.
2) Fuerzas de retención: Al comienzo del ciclo de operación de un PWR, las fuerzas retención son aplicadas a los elementos de combustible. Estas fuerzas se aplican con el fin de comprimir los elementos de combustible para contrarrestar las fuerzas hidrodinámicas y de flotación.
   En este análisis, se ha modelado un dispositivo de retención, y se le aplica esta fuerza al elemento de combustible progresivamente, desde cero hasta su máximo valor.

3) Fuerzas hidrodinámicas: Estas fuerzas son el resultado de la interacción del flujo de refrigerante con la estructura del elemento de combustible.
   Estas fuerzas son modeladas como fuerzas puntuales y superficiales. Por un lado, como fuerzas puntuales para simular las pérdidas de presión del flujo debido a la forma, tanto a la entrada y salida del núcleo, como en cada rejilla espaciadora. Por otro lado, como fuerzas superficiales para simular las pérdida de presión por fricción.

4) Fuerzas térmicas: La expansión térmica de los elementos de combustible tiene una importante contribución en el análisis axial, ya que están sometidos a temperaturas de hasta 400°C. Por ello, en este estudio se han implementado los materiales de cada uno de los elementos, con sus respectivas características que varían con la temperatura. Además, se ha implementado una curva de temperatura acorde con los cambios de temperatura que sufre un elemento de combustible a lo largo del ciclo de irradiación.

5) Fuerzas de fluencia: fluencia lenta y crecimiento por irradiación. El flujo de neutrones dentro del núcleo del reactor provoca la aparición de cargas en las barras de combustible y en los tubos guía.

   - Por un lado, la fluencia lenta por irradiación, es un tipo de deformación dependiente del tiempo, que aparece sólo cuando los elementos se encuentra bajo tensiones mecánicas. Este tipo de deformación se implementa en el modelo como una propiedad de los materiales.
   - Por otro lado, el crecimiento por irradiación tiene lugar en las barras de combustible y los tubos guía a lo largo del ciclo de operación. De la misma forma, se implementa en el modelo como una propiedad de los materiales.

Resultados

Debido a que la fluencia lenta y el crecimiento por irradiación son procesos lentos dependientes del tiempo, su estudio sólo es relevante a lo largo del ciclo completo de irradiación. Por ello, para realizar un análisis axial más exacto del elemento de combustible teniendo en cuenta el impacto de todas las fuerzas que actúan sobre la estructura, el análisis se divide en dos partes: un primer análisis durante la puesta en marcha del ciclo de funcionamiento del PWR, y un segundo análisis a lo largo de todo el ciclo de irradiación. En ambos análisis se estudian los esfuerzos axiales tanto de las barras de combustible como de los

tubos guía, así como la evolución de la fuerza de retención en función del tiempo.

El análisis de los resultados muestra que la variación de los esfuerzos axiales en el modelo del elemento de combustible a lo largo del ciclo de operación coincide con la variación esperada. Además, el crecimiento longitudinal de la estructura debido a las fuerzas axiales existentes en la vasija del núcleo del reactor afecta a la fuerza de retención como se espera.

Los resultados experimentales del análisis axial de un PWR en operación se basan en mediciones realizadas después del ciclo de irradiación. Dichos resultados no proporcionan exactitud ni información sobre los procesos físicos subyacentes. Por ello, la validación de los resultados de este proyecto no se basa en la comparación con resultados experimentales, sino con análisis similares que han sido realizados anteriormente.

Por lo tanto, se puede concluir que, dado que los gráficos obtenidos muestran un gran parecido con estudios similares, el modelo en el que se basa el análisis responde correctamente a las fuerzas axiales que le han sido aplicadas, y por ello es una herramienta fiable para el estudio del crecimiento longitudinal de un elemento de combustible de un PWR.

Sin embargo, dado que este análisis axial se realiza con el fin de estudiar el arqueamiento de la estructura, el estudio estaría incompleto si no se tienen en cuenta las fuerzas laterales y la relajación de los muelles que soportan las barras de combustible. Por ese motivo, se propone la implementación de estos dos análisis en el modelo ya existente para obtener un estudio completo del arqueamiento del elemento de combustible.

Resumen en español

STRUCTURAL ANALYSIS OF THE IRRADIATION-INDUCED LONGITUDINAL GROWTH OF A PWR FUEL ASSEMBLY DURING NORMAL OPERATION USING THE FINITE ELEMENT METHOD

Autor: Isabel Cabrera Millán

Director: Prof. Dr. Rafael Macián-Juan.

Entidad Colaboradora: TUM- Technische Universität München, Lehrstuhl für Nukleartechnik.

PROJECT SUMMARY

Introduction

Pressurized Water Reactors (PWR) are the most widely used nuclear reactors. The main characteristic of this type of reactors is the pressure of the coolant flowing through the first loop that is kept at high levels in order to prevent boiling within the reactor core.

Bow analysis of fuel assemblies is currently an active field of nuclear engineering research because it can lead to both safety and operational problems of the nuclear power plant. However, carrying out experimental tests taking into account all the conditions affecting the operation of a PWR would become an extremely complex task. For that reason, the implementation of a PWR fuel assembly computational model for the bow analysis is needed.

The objective of this thesis is the structural axial growth analysis of a PWR fuel assembly under irradiation as a part of the structure bow study. This analysis is based on a fuel assembly model, which has been implemented in ANSYS using the finite element model.

The figure below shows a typical structure of these fuel assemblies.

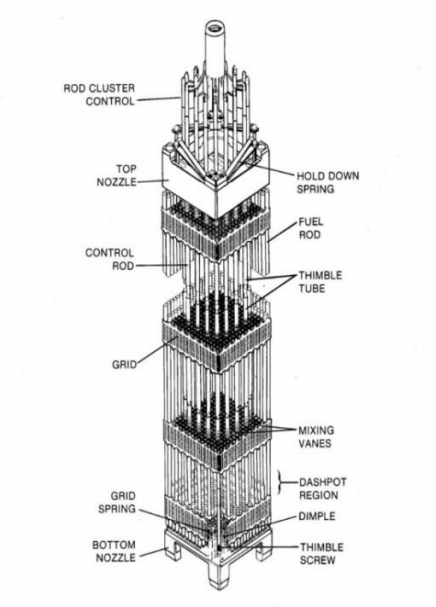

Ilustración 2 Typical PWR fuel assembly

Methodology

For the axial analysis of a PWR fuel assembly, the axial forces that are present in the reactor core during the irradiation cycle have been taken into account.

1) Buoyancy forces: fuel assemblies, which are located within the core vessel, are submerged in the coolant-moderator (water). Therefore, the so called buoyancy forces appear.
   For the work that is presented here, the value of these forces has been calculated and they have been applied as punctual forces at the bottom of each fuel assembly and guide tube.

2) Holddown forces: during the reactor start-up, the holddown forces are applied on the top part of the fuel assemblies. These forces are applied in order to compress the fuel assemblies so that they are prevented from lifting up because of both buoyancy and hydrodynamic forces.
   In this analysis, a holddown device has been modeled and the force is applied to the fuel assemblies in different load steps increasing its value from zero until the maximum value.

3) Hydrodynamic forces: these forces appear as a consequence of the interaction between the coolant flow and the fuel assembly structure.
   Hydrodynamic forces are modeled as punctual and surface forces. On one hand, as punctual forces in order to simulate the flow pressure losses due to the form at both the inlet and the outlet of the core vessel

and also at the spacers grids. On the other hand, they are modeled as surface forces to simulate the friction pressure losses.

4) Thermal forces: thermal expansion of fuel assemblies has an important impact on axial analysis, since they are submitted to temperatures up to 400°C. For that reason, in this study the different materials of which the fuel assembly elements are made of have been implemented with their respective time-dependent characteristics. Furthermore, according to the temperature changes that a fuel assembly undergoes during the irradiation cycle, a temperature curve has been implemented.

5) Fluence forces: These forces are irradiation creep and growth. The neutron flux within the reactor core generates stresses on both fuel assemblies and guide tubes.

   - On one hand, irradiation creep is a time-dependent deformation type that only appears when the elements are under mechanical stresses. This type of deformation is implemented in the model as a material property for the different materials.
   - On the other hand, irradiation growth of fuel assemblies and guide tubes appears over the entire operational cycle. Similarly, they are implemented in the model as a material property.

Results

Since irradiation creep and growth are time dependent processes with a large time scale, the impact of these processes will only be significant over the entire irradiation cycle. For that reason, in order to achieve a more accurate knowledge of the structural axial changes of the fuel assembly, the simulation has been carried out in two parts: a first analysis over the initial start-up of the PWR operating cycle, and a second analysis over the entire irradiation cycle. In these analyses, the axial stresses of both fuel rods and guide tubes are studied. The evolution of the holddown force as a function of the time is also studied.

The analysis of the results shows that the change of the axial stresses in the fuel assembly model over the operating cycle coincides with the expected behaviour. In addition, the longitudinal growth of the structure caused by the axial forces applied in the reactor vessel affects to the holddown force as it was expected.

Experimental results of the axial analysis of a PWR under operation are based on post-irradiation measurements. For that reason, experimental results provide neither accurate information nor insight into the underlying physical processes. Therefore, the validation of the results in this project is not based in the comparison to experimental results, but in the comparison to similar analyses that have been performed.

In conclusion, since the obtained graphs show a good agreement with similar analyses, the fuel assembly model in which this project is based respond correctly to the axial forces that have been implemented, and therefore, it is a reliable tool for studying the longitudinal growth of a PWR fuel assembly.

However, as this analysis is performed as part of a bow analysis, the study would be incomplete without taking into account the lateral forces that appear during the irradiation cycle and the relaxation of the support springs in the grid-to-rod connections. For that reason, the implementation of these two analyses in the model is proposed to be performed in order to obtain a complete study of the fuel assembly bow.

NTech
Lehrstuhl für
Nukleartechnik

Technische Universität München

Master's Thesis

Isabel Cabrera Millán

Structural Analysis of the Irradiation-Induced Longitudinal Growth of a PWR Fuel Assembly during Normal Operation using the Finite Element Method

Betreuer TUM: Prof. Dr. Rafael Macian-Juan

Betreuer: Dipl. -Ing. Andreas Wanninger

Ausgegeben: 01.11.14

Abgegeben: 15.05.15

List of Contents

List of Figures

List of Tables

List of Acronyms

APDL	ANSYS Parametric Design Language
FA	Fuel Assembly
FEM	Finite Element Method
FR	Fuel Rod
GT	Guide Tube
IRI	Incomplete Rod Insertion
PWR	Pressurized Water Reactor
RCCA	Rod Cluster Control Assembly
SS304	Stainless Steel 304
Zry-4	Zircaloy-4

Abstract

Fuel assembly bow is an important issue for nuclear engineering since high bowing levels can lead to operational difficulties that may affect the final performance of the nuclear power plant. However, analyzing PWR bow based only on post-irradiation measurements does not provide insight into the underlying physical processes. Undertaking experimental tests taking into account all representative PWR operation conditions affecting the bow phenomenon would be prohibitively complex. Due to this reason, a computer model of the fuel assembly is imperative for a comprehensive bow investigation.

The purpose of this Master´s Thesis is to perform a structural analysis of the irradiation-induced longitudinal growth of a PWR fuel assembly, as a part of the bow analysis of the assembly. The entire thesis project is based on a finite element model of a typical PWR fuel assembly that has been implemented using ANSYS simulation software.

In this model, the PWR fuel assembly is submitted to all axial forces governing the nuclear reactor performance during operation. Since irradiation creep and growth are time dependent in a large scale, the impact of these processes will only be significant over the entire irradiation cycle. For that reason, in order to achieve a more accurate knowledge of the structural axial changes of the fuel assembly, the simulation has been carried out in two parts. The first simulation has been performed for the initial start-up of the PWR operating cycle and the second one over the entire irradiation cycle. Furthermore, both the axial forces and stresses of several fuel assembly elements have been thoroughly investigated. The results correspond to what was expected from operational experience but still necessitate a thorough validation.

1. General interest of work

1.1 Introduction to pressurized water reactor

The Pressurized Water Reactor (PWR) was developed by Westinghouse based on naval reactor technology, and nowadays this type of nuclear reactors constitute the majority of all western nuclear plants.

The PWR main characteristic is its high pressure inside the vessel. The pressure must be maintained at about 15MPa in order to prevent saturated boiling. Thus, only punctual but not bulk boiling is allowed.

These types of nuclear reactors have three main coolant loops:

- The primary circuit which is in contact with the core.
- The secondary circuit where the steam is produced in the steam generators.
- The third loop corresponds to the condenser loop.

The nuclear core is located inside a pressure vessel which contains the nuclear core and the mechanical support structures (see figure 1.1).

The coolant-moderator enters the vessel through the reactor coolant inlet nozzle, flows down along the down-comer and enters the reactor core from below. It exits the vessel through the outlet nozzle.

The core barrel provides a boundary for the reactor coolant. This barrel directs the reactor coolant flow to the core, and after leaving the core it directs the flow to the outlet nozzles. It is important to safety, because its primary function is to support the core.

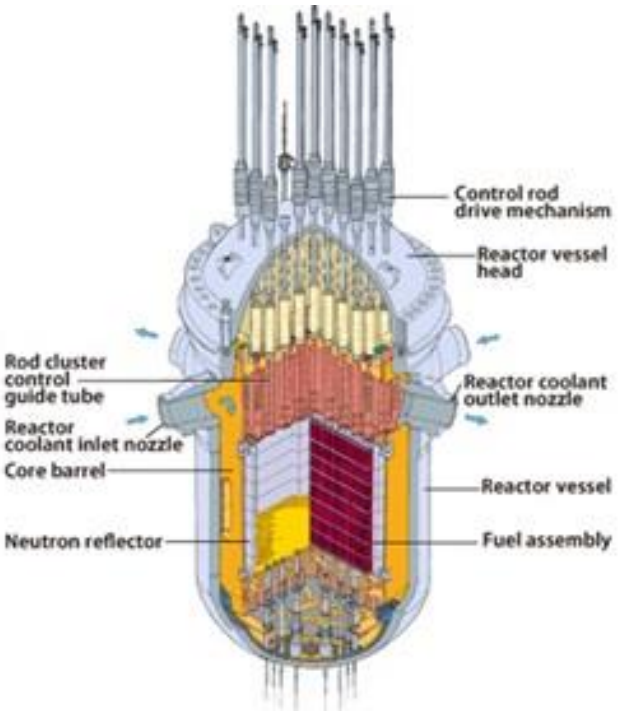

Figure 1.1 PWR pressure vessel [1].

1.2 Description of PWR fuel assemblies

The analysis performed in this paper uses a model that contains the whole structure of a single fuel assembly. For that reason, describing the elements that compose the fuel assembly is of distinctive interest.

In a typical nuclear reactor, the reactor core includes a large number of fuel assemblies. These fuel assemblies contain the fissile material that generates the heat that is removed by the coolant and later used to move the turbines.

Figure 1.2 shows a typical PWR fuel assembly. It consists of a group of cylindrical fuel rods clustered into a square array. These fuel rods are made of ceramic UO_2 pellets with a Zircaloy-4 cladding. However, not all the tubes contain fuel, but also some control rod guide thimbles are placed at selected spaces in the fuel assembly array. The guide tubes are fixed to the top and bottom nozzles of the assembly. The grid assemblies are also fixed to the guide tubes along the height of the fuel assembly in order to hold up the fuel rods, so that they provide support for them in two perpendicular directions.

The bottom nozzle regulates the upward coolant flow and provides fixation at the bottom of the structure. The top nozzle element serves as the upper structural element of the assembly, and directs the coolant flow to the holes in the upper core plate.

The guide thimbles together with the spacer grids and both the bottom and top nozzles constitute the skeleton of the fuel assembly, which is the main load-bearing structure maintaining integrity of the assembly.

The control rod cluster, which is situated at the top of the fuel assembly, is used to start and shutdown the reactor, as well as to control the power during operation and small transients that can occur during the operating cycle.

The holddown springs compress the structure in order to prevent the assembly from lifting due to the upward forces acting during the operating cycle such as hydrodynamic or buoyance forces.

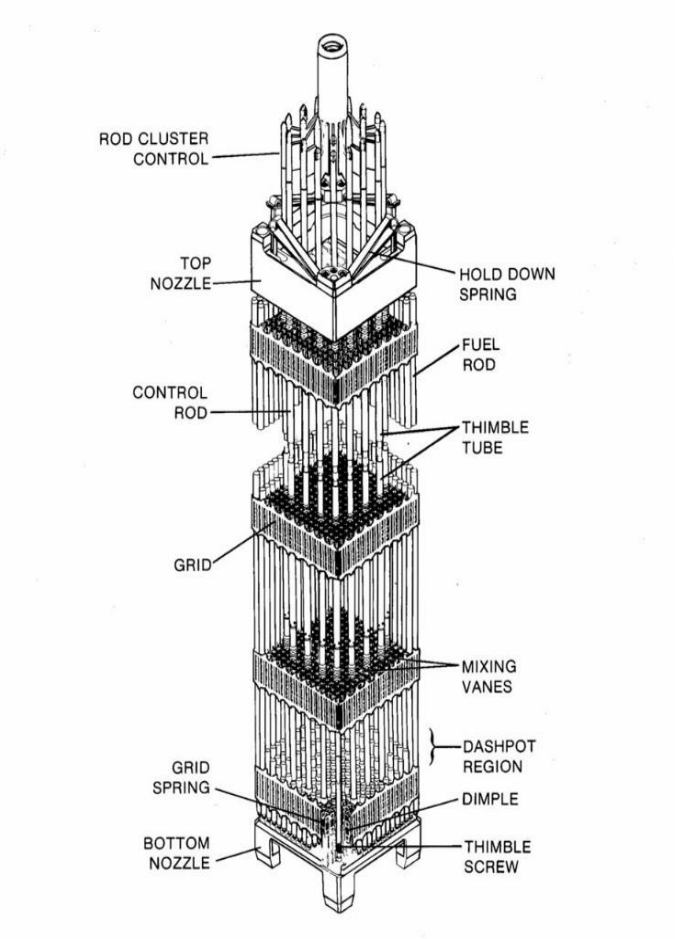

Figure 1.2 PWR fuel assembly [3].

1.3 Framework of the project: bow analysis

The fuel assembly bow is an important issue since extreme bowing levels can lead to some difficulties that may affect the nuclear plant performance. This bow, often with an S-shape but also C-shape (see Figure 1.3), has been observed in certain fuel designs. Thus, the prediction of the mechanical behaviour of the fuel assembly under irradiation is essential in order to minimize the damage that can be caused by excessive deformation of the structure. For that reason, the fuel assembly bow is a very active field of research, and therefore the improvement of bow modelling instruments has become very important within the last decade.

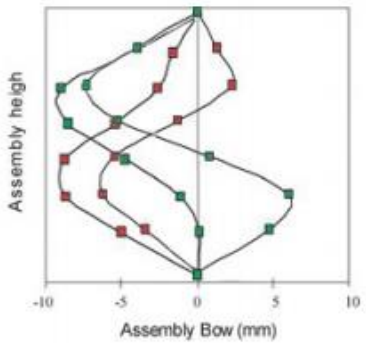

Figure 1.3 Example of fuel assembly bow [4].

Several problems in the fuel assembly can arise from high element deformation levels during operation. Examples of these problems include: increased control rod drop time, incomplete rod insertion (IRI) events, and formation of water gaps that can cause power or flow redistribution. Additionally, the fuel assembly bow can lead to contact with neighbouring fuel assemblies, consequently causing the appearance of high friction forces between them. This contact may result in a connection with vibration, and can origin wear or even perforation at the corners of the spacer grids of neighbouring assemblies. Therefore, the fuel assembly bow is not only relevant regarding safety (increased rod cluster control assembly (RCCA) drop time), but also regarding power distribution (formation of water gaps).

Excessive holddown forces, relaxation of the fuel assembly due to irradiation creep and irradiation growth appear to be important contributors to the structure bow.

It is not easy to perform a bow analysis directly to a real fuel assembly of a nuclear reactor since a test cannot be done taking into consideration all the representative PWR conditions. For this reason, a computer model of the fuel assembly is required in order to perform a more accurate bow study. Hence, a finite element beam model is used as the basis of the mechanical bow behaviour of a fuel assembly.

1.4 Axial analysis as part of bow analysis

During operation, the fuel assembly is submitted to different axial forces that govern the nuclear reactor performance. The magnitude of these forces depends on the reactor design, the material used in elements, power gradients, etc. and their presence in the fuel assembly which can contribute to a certain amount of bow in the structure.

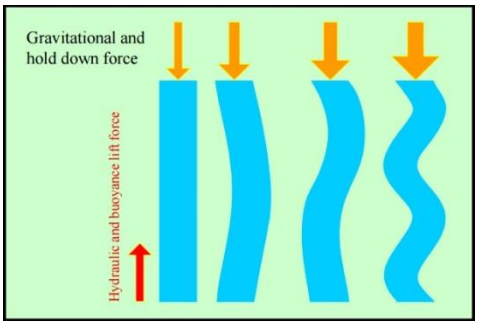

Figure 1.4 Schematics fuel assembly bow. The second, third and fourth drawings show B-shape, S-shape and W-shape mode of bowing, respectively [5].

The aim of this study is to analyse separately the effect of the axial forces inside the fuel assembly, and afterwards to simulate a complete operating cycle of a nuclear reactor taking all the forces into account. The axial forces that are going to be modelled and studied are:

1) Buoyancy forces: these forces appear due to the fact that the fuel assembly is submerged in the coolant during the operating cycle. They are not particularly relevant, as their magnitude is not high in comparison to the rest of the forces, but it is necessary to take them into account in order to perform a complete axial analysis.

2) Holddown forces: Axial compression from holddown springs restricts free axial growth of the assembly during irradiation. These forces are applied to the structure at the beginning of the operating cycle, before the start-up of the pumps, in order for the fuel assembly not to lift due to the effect of the

hydrodynamic forces. Excessive hold-down forces often contribute significantly to the fuel assembly bow.

3) Hydrodynamic forces: The coolant flows from the bottom part of the assembly to the top part, recollecting the heat generated by the fissions. The water flow generates hydraulic forces all along the height of the fuel assembly. The effect of these forces should be counteracted by the holddown forces.

4) Thermal expansion: The nuclear reactor core is submitted to elevate temperatures during its operating cycle as a result of the heat released in the fissions. Consequently, the elements of the fuel assembly suffer a thermal expansion, causing a growth on the length of the structure that should be absorbed by the holddown forces.

5) Irradiation creep and growth: both irradiation creep and irradiation growth are relevant processes for anisotropic materials such as Zircaloy-4. For zirconium-base alloys, thermal creep, irradiation creep and irradiation growth are the main ways of deformation.

- Creep refers to a time dependent deformation of elements under load. Within the reactor environment, due to the production of excess defects, irradiation accelerates creep.
- Irradiation growth refers to a volume conservative distortion that appears in the elements without external stresses but due to the fast neutron fluence in the fuel assembly.

Since guide tubes and the cladding of the fuel rod are made of Zircaloy-4, these processes are relevant and they need to be taken into account.
Thus, the fuel assembly length increases because of the irradiation growth and oxide formation, and decreases due to creep and elastic formation.

1.5 Operating cycle of a PWR

How the axial forces are implemented in the ANSYS model is explained in chapter 3. These forces are finally applied to the fuel assembly step by step simulating thus a real operating cycle, which has the following phases:

1. Water filling: The appearance of the buoyance forces is simulated with a water filling of the core vessel where the fuel assemblies are located. Actually, in real PWR operating cycle, the vessel is already filled with the coolant, and the fuel assemblies are introduced into the vessel at the beginning of the cycle.
2. Vessel closure: The upper core plate pushes the holddown springs and compresses the fuel assemblies.
3. Start-up of pumps: Hydrodynamic forces appear in the structure due to the coolant flow.
4. Transition to hot conditions: Addition of the thermal expansion effect on the different fuel assembly elements.
5. Irradiation stage: In this stage, the PWR is under nominal conditions. Irradiation causes creep and growth effect in guide tubes and fuel rods.
6. Return to cold conditions: Thermal contraction of the materials due to the decrement of the temperature within the reactor.
7. Stopping of pumps: Hydrodynamic forces are not exerted in the fuel assemblies any more.
8. Vessel opening: The compressive holddown force disappears.

2. Modelling approaches

2.1 ANSYS mechanical APDL

ANSYS is recognized as the most powerful engineering design analysis software. It is used for performing finite element analysis (FEA) of mechanical parts or fluids.

APDL –ANSYS Parametric Design Language- is the primary language used to communicate with the ANSYS mechanical APDL solver. This scripting language can be used to automate common tasks or even to build a parametric model. APDL encompasses a wide range of other features, such as if-then-else constructs, do-loops, and vectors and matrix operations.

ANSYS mechanical APDL software can build two –or three- dimensional models, apply loads, obtain solutions and display results.

A finite element analysis in ANSYS is normally done in three main stages:

1) Preprocessing: Definition of the problem.

    - Definition of the materials and material properties.
    - Definition of geometric data of the elements.
    - Elements definition and keyoptions.
    - Node and element positions.
    - Definition of structural constraints.

2) Solution:

    - Definition of the different load steps and solving.

3) Postprocessing:

    - Lists of nodal solutions such as nodal displacements.
    - Lists of element solutions such as structural forces and moments, or element stresses.
    - Plots and diagrams.

2.2 Important finite elements in the model

The basis of this project is a fuel assembly model in ANSYS (see figure 2.1), from which the axial analysis is performed. This model is mainly composed of beams and springs, elements that will be briefly described in order to better understand the analysis.

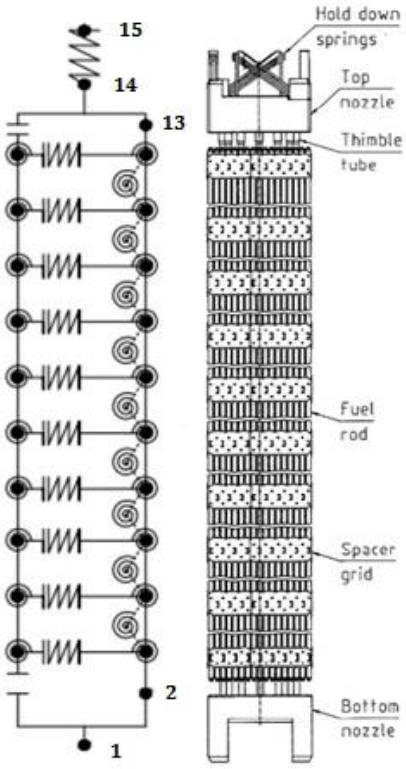

Figure 2.1 Typical PWR fuel assembly (right) and simplified beam model (left) [6].

The guide tubes and fuel rods are modeled by vertical beams, as shown schematically in figure 2.1 above. Both guide tubes and fuel rods are modeled with the same beam element (Beam 188), but with different geometric properties depending on their mechanical characteristics. The spacer grids are modeled as a system of different springs and kinematic constraints (grid-to-rod or grid-to-thimble connections) evenly distributed throughout the height of the fuel assembly. A non-linear spring is used to model the holddown spring at the top of

the fuel assembly. The model is completed by the top and bottom nozzles that are modeled by beams.

The most important ANSYS elements used in the model when an axial analysis is performed are:

- **<u>BEAM 188</u>**

This element is suitable for the analysis of thin or moderately thick beam structures. It supports linear as well as nonlinear analyses, including plasticity, large deformation and nonlinear collapse.

The BEAM188 is used in the model for the fuel rods and guide tube elements, and its main characteristics are:

- It is a linear, quadratic, or cubic two-node beam element in 3D.
- It has six degrees of freedom at each node (UX, UY, UZ, ROTX, ROTY, ROTZ)
- The section geometry of the element can be defined by the user. In this model, an equivalent rectangle section is used for the fuel rods and guide tubes, and a hollow rectangular section for the top and bottom nozzles.
- Regarding the loads that are applied in the element:

- Forces are applied at the nodes.
- If the centroidal axis is not collinear with the element x-axis, applied axial forces will cause bending.
- Pressures can be input as surface loads on the element faces.
- Lateral pressures are input as force per length unit.
- Temperature can be input at both ends of the elements.

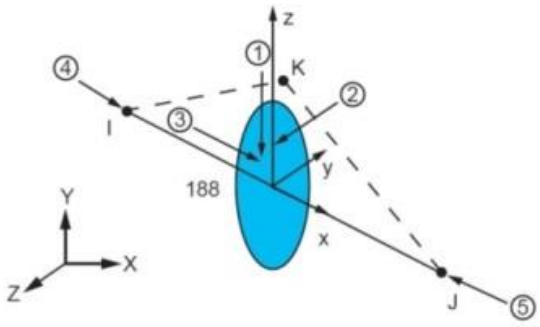

Figure 2.2 Beam188 Geometry [7].

- **COMBIN 39**

This element is a nonlinear spring used to model the hold down spring. COMBIN39 is a unidirectional element with nonlinear generalized force-deflection capability that can be used in any analysis. Its main characteristics are:

- The element is defined by two (preferably coincident) node points, and a generalized force-deflection curve.

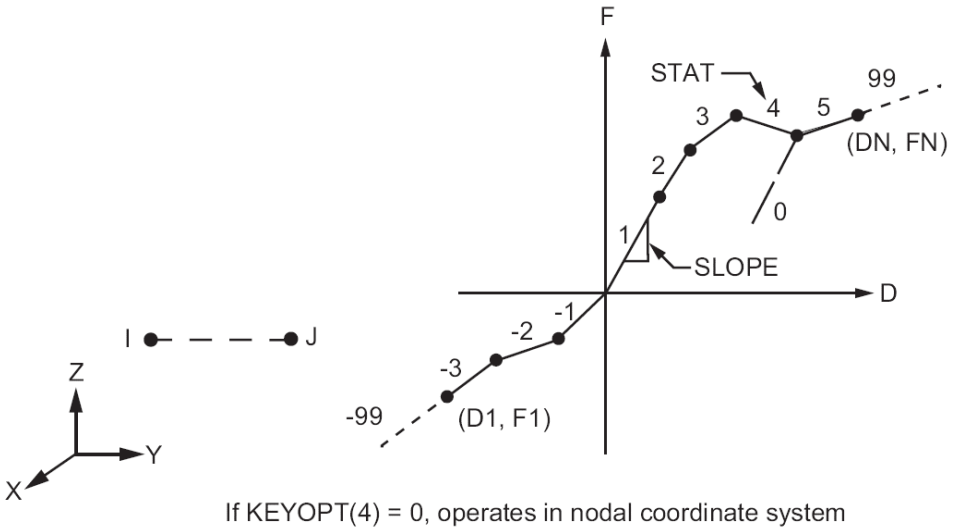

Figure 2.3 Combin39 Geometry [7]

The points on the foregoing curve (D1, F1, etc.) represent force (or moment) versus relative translation (or rotation) for structural analyses.

- The element has longitudinal or torsional capability in 1D, 2D or 3D applications. The longitudinal option is a uniaxial tension-compression element with up to three degrees of freedom at each node (UX,UY,UZ).
- The element has no mass.
- No surface or body loads.
- The element has large displacement capability for which there can be two or three degrees of freedom at each node.

- **MPC 184**

The MPC184 rigid link/beam element can be used to model a rigid constraint between two deformable bodies or as a rigid component used to transmit forces and moments in engineering applications. In this model, the MPC184 is used to

model the spacer grids and the main pin of the hold down device, through which the force from the upper core plate is applied to the structure.
Its main characteristics are:

- Two nodes define the element.
- If the keyoption 2 of this element equals 1, the Lagrange multiplier method is chosen, and therefore the MPC184 can also be used in applications that call for thermal expansion on an otherwise rigid structure. In this model, the keyoption 2 equals 0 for the spacer grids since the thermal expansion of these elements is not relevant for the axial analysis of the fuel assembly. For the main pin of the holddown device, keyoption 2 equals 1, and the thermal expansion coefficient of the material is given as an input to the program.
- Density must be specified if the mass of the rigid element is to be accounted for in the analysis. If density is specified, ANSYS calculates a lumped mass matrix for the element.

3. Axial analysis of a fuel assembly

3.1 Buoyancy forces

3.1.1 Introduction

The core vessel of a PWR is filled with the coolant (water), which is used to collect the heat generated by the fissions of the Uranium^{235}. When the fuel assemblies are introduced into the vessel, the so-called buoyancy forces appear.

3.1.2 Definition

When an object is totally or partially submerged in a liquid, an upward force called the buoyancy force appears. This force equals the weight of the fluid displaced by the object. Moreover, this weight is proportional to the volume of the mentioned displaced fluid if the density of the fluid is uniform.

Thus, the magnitude of the force is determined by the following formula, in the opposite direction to gravity:

$$Buoyancy\ Force = \rho_{Fluid} \times Volume_{Object} \times gravity \qquad Equation\ 3.1$$

The force distribution is shown in Figure 3.1.

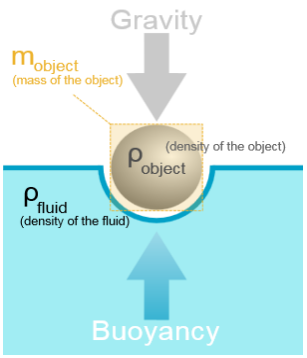

Figure 3.1 Force distribution of a submerged object.

According to figure 3.1, all the elements of the fuel assembly which are located inside the reactor's vessel, and therefore immersed in the coolant, create an upward force in the opposite direction to gravity.

3.1.3 Model description

These forces are modelled as punctual forces, which are applied at the bottom of each guide tube and fuel rod element. It is considered in this analysis that only these elements generate buoyancy forces.

In order to model the buoyance forces, the calculation of their value is necessary, following equation 3.1. For this axial analysis, the density of the water is used, and the value of the gravity is assumed.

Regarding the elements volume, both guide tubes and fuel rods:

- Volume of fuel rods:

The fuel rods are closed at both ends as they are filled with the fuel pellets and filling gas, so their displaced volume approximates to the volume of a cylinder, taking the external radius of the clad as the radius of the cylinder.

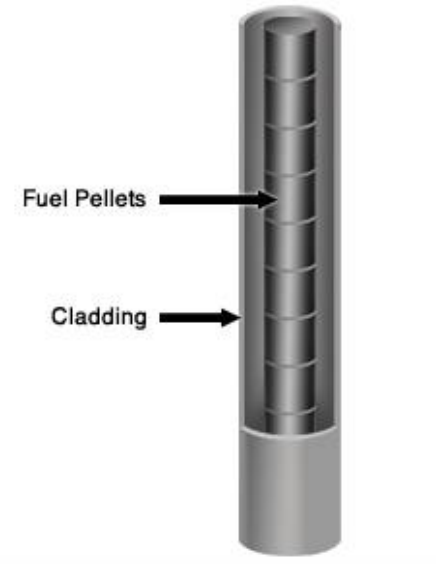

Figure 3.2 Configuration of a PWR fuel rod [10].

Thus, the equivalent volume of a single fuel rod is calculated as:

$$V_{Fuel\ Rod} = {r_{out,FR}}^2 * \pi * H_{Fuel\ Rod} \qquad \textit{Equation 3.2}$$

Where:

$r_{out,FR}$: Outer radius of the fuel rod cladding.
$H_{Fuel\ Rod}$: Height of a fuel rod.

- Volume of guide tubes:

Guide thimbles are hollow tubes that are distributed throughout the fuel assembly array, extending longitudinally between the bottom and the top nozzles. They provide stiffness to the structure and serve as guide to the control rods which are inserted into the fuel assembly during operation in order to increase or decrease the power level of the reactor.

Moreover, the lower portion of the guide thimbles serves as a hydraulic brake (dashpot) for the control rods (see figure 1.2). If the nuclear reactor power needs to be decreased drastically, the control rods are allowed to fall quickly into the fuel assembly, but this fall should be controlled in order not to cause additional damage. For that reason, the reduction of the inner diameter in the lower part of each guide tube makes the upward flowing coolant become trapped by the entering control rod, and therefore this functions as a dashpot that decelerates and brakes the control rod.

Thus, in order to calculate the equivalent volume of the guide tubes immersed in the coolant, it is necessary to take into account the fact that they are hollow, and also that the lower part of each one is thicker due to dashpot.

The volume of one guide tube can be calculated as:

- Volume of the dashpot part:

$$V_{Guide\ Tube,dashpot} = ({r_{out,GT}}^2 - {r_{inn,dashpot}}^2) * \pi * H_{Dashpot} \qquad \textit{Equation 3.3}$$

Where:

$r_{out,GT}$: Outer radius of the guide tube.
$r_{inn,dashpot}$: Inner radius of the guide tube in the dashpot part.

$H_{Dashpot}$: Height of the dashpot part in the guide tube.

- Volume of the guide tube without the dashpot part:

$$V_{Guide\ Tube,NOdashpot} = \left(r_{out,GT}{}^2 - r_{inn,GT}{}^2\right) * \pi * H_{GT,NOdashpot} \qquad \textit{Equation 3.4}$$

Where:

$r_{inn,GT}$: Inner radius of the guide tube.
$H_{GT,NOdashpot}$: Height of the guide tube minus the height of the dashpot part.

Then the total volume of one guide tube is:

$$V_{GT} = V_{Guide\ Tube,dashpot} + V_{Guide\ Tube,NOdashpot} \qquad \textit{Equation 3.5}$$

Once the volumes are calculated, and together with the value of the density of both the water and the gravity, the magnitude of the buoyancy forces can be estimated:

- ✓ F_{BUO-GT}
- ✓ F_{BUO-FR}

These values correspond, respectively, to the magnitude of the buoyancy forces that appear due to the immersion of the guide tubes and fuel rods in the coolant during operation.

3.2 Holddown forces

3.2.1 Definition

During the operating cycle of the nuclear reactor, the fuel assemblies are subjected to the upward forces exerted by the cooling flow. For that reason, retaining the fuel assemblies in place is important. Moreover, the assemblies undergo dimensional changes over time, which are produced mainly by the irradiation growth and creep effect. Thus, the holddown springs must be able to provide the structure with a suitable holddown force in order to counteract the hydrodynamic forces while absorbing the change of the fuel assembly height.

Therefore, the aim of the holddown device is to prevent the whole structure to lift due to the effect of the upward forces of the coolant, while at the same time allowing the structure to grow because of the thermal expansion.

Nevertheless, it is also important to take into account that high forces can lead to excessive bowing of the fuel assembly because of the axial compression load on the top of the assembly.

3.2.2 Physical explanation

For the present study, holddown springs as used for German-type PWR fuel assemblies are considered, as shown in figure 3.3.

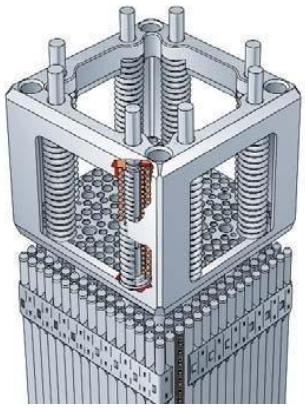

Figure 3.3 Typical Holddown springs used for German-type PWR [11].

The holddown springs are located at the upper part of the fuel assembly. As shown in figure 3.3, the spring elements, which are mounted in the fuel assembly head, protrude from the structure on both sides of each corner of the fuel assembly head for elastic supporting of the frame at the non-illustrated upper core plate.

The holddown spring is initially preloaded with the following load value:

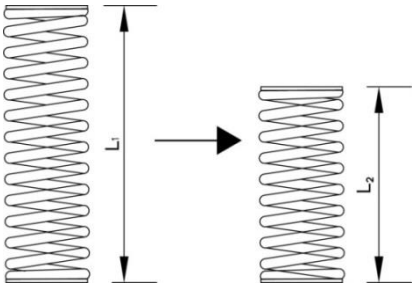

Figure 3.4 Compression of the holddown spring from L1 to L2

$$F_{PRELOAD} = K_{Hold-down\ spring} * (L_1 - L_2) \qquad \textit{Equation 3.6}$$

L_1 is the original length of the spring, and L_2 is the length of the initially compressed spring, which is also indicated in figure 3.5.

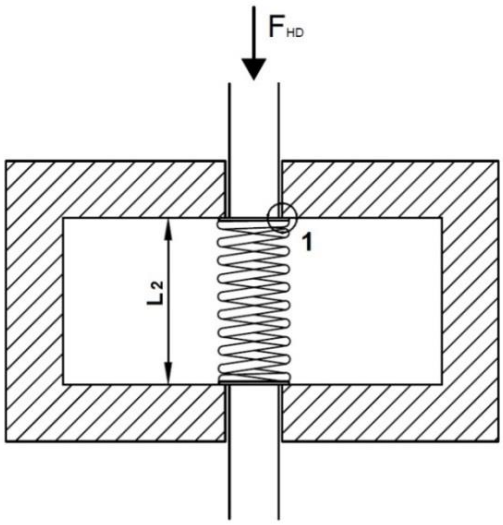

Figure 3.5 Schematic cross section of the holddown device mounted in the fuel assembly head

In figure 3.5, a schematic cross section of the fuel assembly head is shown. The conventional spring element is formed from a pin which is slidably mounted in bores provided in the fuel assembly head. Hence, the upper pin represents the pin through which the holddown force is transmitted, whereas the lower pin in the figure symbolizes a guide tube. The mechanical connection between the spring and the upper bar of the head is highlighted in part 1.

F_{HD} represents in figure 3.5 the direction of the holddown force applied from the upper core plate which has a value of zero at the beginning.

The initial distribution of forces is shown schematically in figure 3.6.

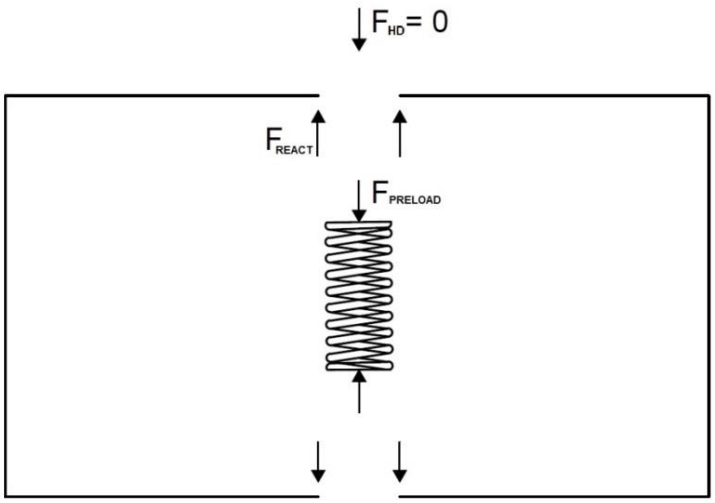

Figure 3.6 Initially force distribution of the holddown spring and the fuel assembly head

At the beginning, the holddown spring is compressed, and the reaction force (F_{REACT}) equals the preload force. The system is in equilibrium, and no force is transmitted to the fuel assembly.

At a certain moment, the upper core plate starts to compress the pin that is connected to the spring, and, as a result, the value of the holddown force is not zero anymore, and starts to increase.

At this point, the process can be separated in two different stages:

Stage 1: The holddown force from the upper core plate exerted on the structure is lower than the *preload* force of the spring:

$$F_{HOLDDOWN} < F_{PRELOAD}$$

In this case, the force is transmitted to the fuel assembly through the upper bar of the head, since there is still a mechanical connection between the upper bar of the head and the spring.

As the spring has to be in equilibrium, the following equation has to be fulfilled.

$$F_{PRELOAD} = F_{REACT} + F_{HOLDDOWN} \qquad \textit{Equation 3.7}$$

According to equation 3.7, as the holddown force increases, the reaction force in the structure through the connection point decreases, since the preload force is constant.

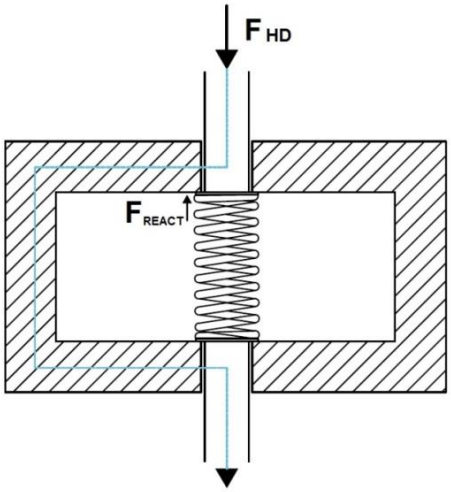

Figure 3.7 Schematic cross section of the holddown device mounted in the fuel assembly head with the force transmission path during the first stage.

Thus, the increasing holddown force is transmitted to the fuel assembly by the decrease of the reaction force exerted on the upper bar of the head as shown in figure 3.7. The elastic stiffness $K1$ resisting this part of the compression hence equals the stiffness of the fuel assembly structure.

Stage 2: The holddown force from the upper core plate exerted in the structure is higher than the preload force of the spring.

$$F_{HOLDDOWN} \geq F_{PRELOAD}$$

According to equation 3.7, when the holddown force equals the preload force, the reaction force becomes zero, and, as a consequence, the mechanical connection between the spring and the head of the fuel assembly disappears.

In this stage, the holddown force is directly transmitted to the fuel assembly through the spring (see figure 3.8). The elastic stiffness $K2$ resisting this part of the compression hence corresponds approximately to the spring stiffness. This can be explained by the fact that the stiffness of the spring and the fuel assembly structure, respectively, are in series, and therefore, as the stiffness of the FA

structure is considerably higher than the one of the spring, the first one can be neglected.

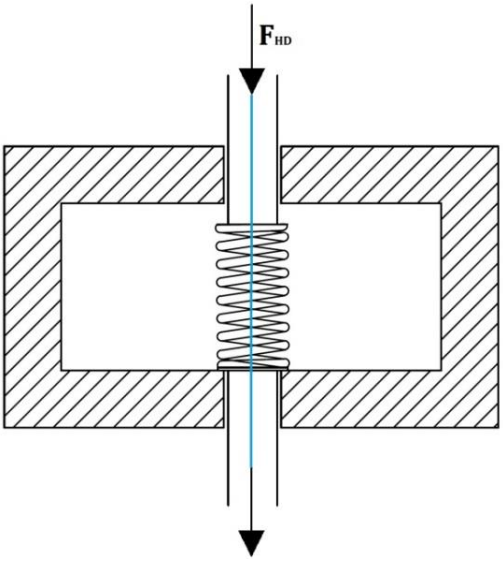

Figure 3.8 Schematic cross section of the holddown device mounted in the fuel assembly head with the force transmission path during the second stage.

In figure 3.9, which shows the theoretical evolution of the axial holddown load as a function of the axial deflection of the top nozzle, the two different stages can be observed.

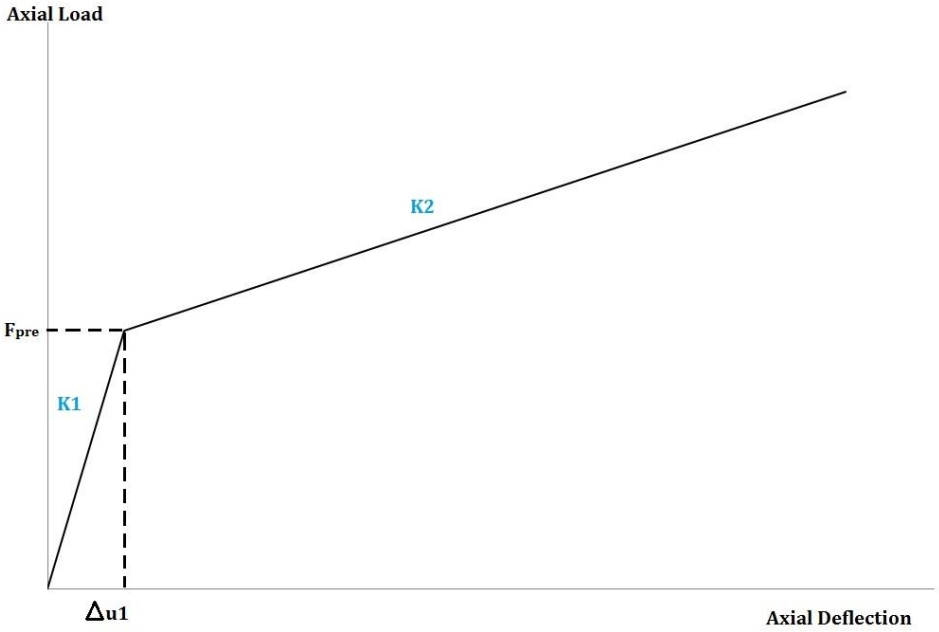

Figure 3.9 Graph- Axial load vs Top nozzle axial deflection

Where:

$K1$: Stiffness of the fuel assembly structure.

$K2$: Approximates stiffness of the hold-down spring.

F_{pre}: Preload force

Δu_1: Displacement of the top nozzle due to the axial load applied on the pin, according to the stiffness of the fuel assembly structure.

3.2.3 Model description

A simplified model of the physical behavior of the holddown device is simulated with the COMBIN39 element (see section3.2.2).

The advantage of this COMBIN39 element is that its nonlinearity can be used to model the change in the slope as shown in figure 3.9, simulating thus the change in stiffness while applying the holddown force. The use of this element needs the input of the force-deflection curve, and therefore the points where the slope must change.

Moreover, not only the spring but also the main pin of the holddown device needs to be modelled. The ANSYS element used to model the pin is the MPC184, thus neglecting its elasticity. The material used in this element is important since the fuel assembly is subjected to elevated temperatures, and therefore the thermal expansion of each element is relevant in axial analysis terms. A typical material for the holddown device is Inconel X-750.

Thus, the hold down device of the fuel assembly is modelled by the COMBIN39 in order to model the two stages that have been described previously, and by the MPC184 element to model the pin where the force is applied. The resulting element is shown in figure 3.10.

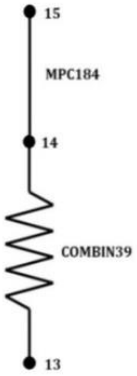

Figure 3.10 Schematic holddown device representation in ANSYS

The node 13 is connected to the lower node of the fuel assembly head, and the node 15 is the top part of the hold down pin, where the force is applied.

3.2.4 Results

Once the element has been modeled, a force is applied progressively to the hold down device in the top node of the element (node 15). This force is created with a progressive compression of the structure.

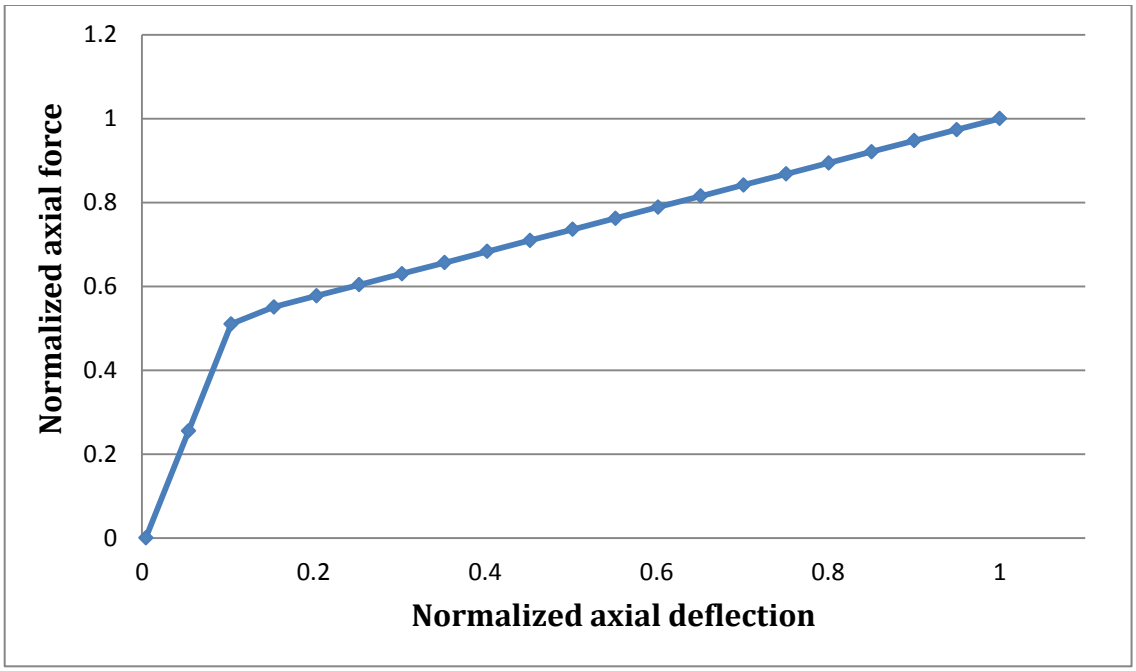

Figure 3.11 Graph- Simulated Axial load vs. Top nozzle axial deflection

In the model, the displacement in node 15 is progressively applied, and the resulting force is observed. This resulting axial force is transmitted to the fuel assembly, and compresses it. The compression of the assembly causes negative stresses in the structure, which have higher values in the guide tubes than in the fuel rods due to the fact that the force is directly applied to the guide tubes.

Figure 3.11 follows the theoretical curve of figure 3.9, which means that the COMBIN39 element represents a suitably simplified model of the physical behavior of the holddown device.

3.3 Hydrodynamic forces

3.3.1 Introduction

In a PWR, the coolant-moderator (water) enters the core vessel through the inlet nozzle, flows down the downcomer and enters the fuel assembly from below. The water is used to collect the heat released by the fissionable material inside the fuel rods, flowing from the bottom part of the fuel assembly to the top part and leaving the nuclear core through the outlet nozzle at an elevated temperature.

The hydraulic lift force of a fuel assembly is the resultant force of the interaction between coolant flow and the fuel assembly.

3.3.2 Model description

The pressure drop of the rod bundle generates hydromechanics forces. Several mechanisms will cause a pressure drop along the coolant channel under nominal operating conditions:

1. Friction pressure drop from the fuel rod bundle (channel friction).
2. Form losses from the spacer grids used to maintain fuel assembly geometry.
3. Pressure losses at the core inlet and exit flow plenum (contraction or expansion).

Thus, the hydrodynamic forces have been modelled as both friction forces and punctual forces in guide tubes and fuel rods.

- Friction forces: This component of the hydraulic forces due to the friction losses within a flow channel is modelled in guide tubes and fuel rods as surface loads with the SFBEAM command. These friction losses are caused by the viscous friction of the fluid with the solid walls of the channel, and are assumed to have the same value for both guide thimbles and fuel tubes.

- Punctual forces: In order to model the form pressure losses of the coolant flow along the fuel assembly, punctual forces at every grid level are added, as well as at the bottom and top nozzles. These form losses are due to the presence of spacer grids in the fuel assembly, and because of the contraction or expansion of the fluid at the entrance and exit of the fuel assembly.

  They are applied with the F command, and are considered to be evenly distributed along the intermediate spacer grids (from 2^{nd} to 8^{th}), and have appropriate values for the lowest and highest grids, as well as for the bottom and top nozzles, according to the form pressure losses at these levels.

3.4 Thermal expansion

3.4.1 Introduction

The material properties of the elements play an important role in a nuclear reactor since it is subjected to elevated temperatures during operation. For that reason, the materials used in these elements should have strong properties from ambient temperature up to 400°C under normal operating conditions in order to achieve a stable performance of the nuclear power plant during the entire operational cycle.

Therefore, taking into account that the effect of the thermal expansion cannot be neglected against the hydrodynamic forces, the buoyancy forces or the hold down forces, considering the thermal expansion in the axial analysis of forces in the fuel assembly is required.

3.4.2 Definition of materials properties

1) Zircaloy-4.
   This is a zirconium alloy used for the guide tubes and for the cladding of the fuel rods.
   The Zircaloy-4 has an excellent corrosion resistance, good mechanical properties and a low thermal neutron cross section. Additionally, regarding its

thermal properties, it is considerably better than other traditional materials: Zircaloy-4 has thermal conductivity which is 30% higher than stainless steel and its linear coefficient of thermal expansion is nearly one-third the stainless steel value. For that reason, Zircaloy-4 is more stable at high temperatures.

2) Stainless Steel 304.
   This material is used for the foot and head of the structure, and for the core barrel (see figure 1.1).
   The stainless steel has good mechanical properties such as strength, durability and also non-corrosive properties.

3) Inconel X-750.
   It is used in the hold down springs, since springs should be made of materials with low stress relaxation rates such as Inconel X-750.
   The Inconel X-750 is a precipitation hardenable nickel- chromium alloy, which is used due to its corrosion and oxidation resistance as well as its strength at elevated temperatures, in addition to its economics and its availability.

The values of the material properties used in the model are shown in table 3.1.

Material	**E modulus at 20°C (GPa)**	**E modulus at 316°C (GPa)**	**Thermal expansion coeff. 20°C – 330°C (m/mk)**
Zircaloy-4	94.5	77	5.5 e-6
SS 304	193	171	1.73 e-5
Inconel X750	214	198	1.35 e-5

Table 3.1 Properties of the fuel assembly materials [13], [14], [15], [16].

The foregoing table shows a comparison between the properties of the three materials. The Inconel X-750 and the Stainless Steel 304 expand more than the Zircaloy-4, as the value of their thermal expansion coefficient is substantially higher than the one of the Zircaloy-4. Moreover, while comparing the values of the

Young's modulus, it can be observed that the Inconel X-750 and SS304 are stiffer than Zircaloy-4.

3.4.3 Model description

In order to model all these material properties, and the change of the values with the change in the temperature, MPDATA and MPTEMP commands have been used.

- **MPTEMP** command defines a temperature table for the material properties.
  It is modeled as MPTEMP,STLOC,T1,T2,T3,T4,T5,T6 where STLOC is the starting location in table for entering temperatures, and from T1 to T6 are the temperatures assigned to six locations.
- **MPDATA** command defines property data to be associated with the temperature table.
  It is modeled as MPDATA,Lab,MAT,STLOC,C1,C2,C3,C4,C5,C6 where Lab is the label corresponding to the type of material property that is going to be defined, MAT is the reference number of the material, STLOC is the starting location in the table for generating data, and C1 to C6 are the property data values assigned to six locations.

With these two commands, the material properties can be defined among a wide range of temperatures. In this case, the Young's modulus should change with the temperature. Thus, two values of the E modulus for two different temperatures are given, and the rest values for intermediate temperature values are interpolated by the program.

TEMPERATURE PROFILE

Figure 3.12 shows the temperature evolution of the nuclear reactor core along the operating cycle, which is modeled following these steps:

1. Ambient Temperature of 20°C at the beginning of the cycle
2. Cold start-up, at a temperature of 50°C.
3. Hot start-up, at a temperature of 300°C.
4. Nominal power operation. Curve shown in figure 3.13.
5. Hot shutdown, at a temperature of 300°C.
6. Cold shutdown, at a temperature of 50°C.

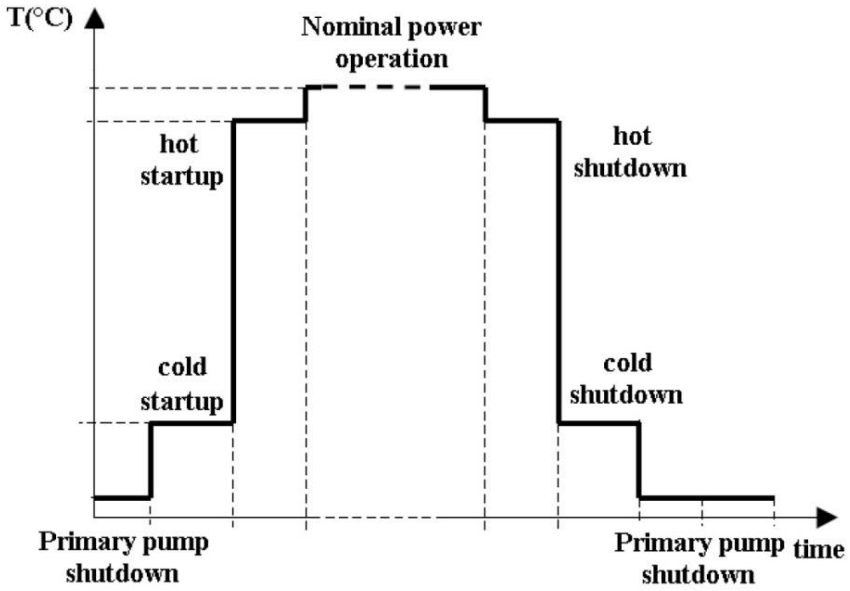

Figure 3.12 Temperature profile during a PWR operating cycle [17].

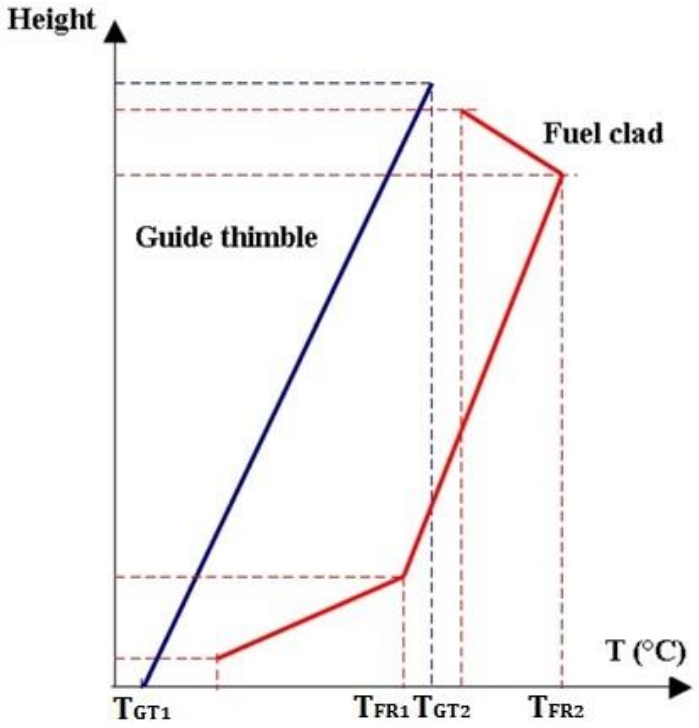

Figure 3.13 Temperature profile of guide tubes and fuel rods during nominal operation [17].

During nominal power operation (see figure 3.13), the temperature of the fuel assembly increases with the height, as the coolant enters the structure from below, and it increases its temperature as it flows up. The temperature of the fuel

clad is higher than the temperature of the guide thimble since the heat comes from the fission reactions inside the fuel pellets.

The temperature values assumed in this temperature profile during the operating cycle have been:

- For the guide tubes:
  - Core inlet temperature (temperature at minimum height): 292 °C (see T_{GT_1} in figure 3.13).
  - Core outlet temperature (temperature at maximum height): 326 °C (see T_{GT_2} in figure 3.13).
- For the fuel clad:
  Different temperature profiles within a reasonable range have been assumed in order to analyze how the stresses of the elements in the structure change.
  - Profile 1:
  - Minimum height fuel rod: 320 °C (see T_{FR_1} in figure 3.13).
  - Maximum height fuel rod: 340°C (see T_{FR_2} in figure 3.13).

  - Profile 2:
  - Minimum height fuel rod: 350°C (see T_{FR_1} in figure 3.13).
  - Maximum height fuel rod: 380°C (see T_{FR_2} in figure 3.13).

Both profiles for the fuel clad include temperatures higher than the ones assumed for the guide tubes. In each case, the temperatures for the minimum and maximum height are given, and for the ones in the intermediate levels the values are interpolated.

In the model, the material properties have been defined and each temperature step within the operating cycle has been simulated in order to see how the fuel assembly reacts to the temperature changes.

The core barrel (see figure 1.1) encloses the nuclear core. It is made of SS304, and under hot conditions its displacement due to thermal expansion is substantially higher than the displacements of the fuel assembly, which is made mainly of Zircaloy-4. This difference in the thermal expansion between the core barrel and the fuel assembly generates an axial decompression of the fuel assembly, and consequently, the holddown force decreases. This elongation of the fuel assembly is modeled by adding a positive displacement to the fuel assembly.

3.4.4 Results

Initially, a theoretical study has been made in order to compare these results to the results given by ANSYS simulation software.

- **ANALYTICAL RESULTS**.

As explained before, three different materials are used in the fuel assembly; therefore, the expansion of these materials have to be calculated separately for each temperature step.

$$\Delta u_{x,SS304} + \Delta u_{x,ZRY4} + \Delta u_{x,INCONEL-X750} \qquad \textit{Equation 3.8}$$

Δu_x is the axial displacement of the structure and in each case is equal to:

$$\Delta u_x = \alpha_{material} * \Delta T * H \qquad \textit{Equation 3.9}$$

Where:

- $\alpha_{material}$ is the thermal expansion coefficient of the material.
- ΔT is the difference between the current temperature and the reference temperature. ($T - T_{REF}$).
- H is the height.

In order to calculate the axial expansion due to thermal loads, the relative elevation of the elements of the fuel assembly is needed.

Elements	Elevation (m)	Node
Top of Hold Down springs	4.877	15
Top of Head	4.827	14
Guide Tube- Head	4.646	13
Foot- Guide Tube	0.181	2
Lower core plate – foot	0	1

Table 3.2 Height of the fuel assembly elements [19].

Table 3.2 shows the elevation values that have been used in the model, and the corresponding nodes (see figure 2.1 in section 2.1). Thus, the height of each element is:

H_{FOOT} = H_{HEAD} = 0.181 m.

$H_{GUIDE\ TUBES}$ = 4.465 m.

$H_{HD\ SPRING}$ = 0.231 m.

The height of the hold down spring includes the height of the fuel assembly head since the spring is mounted in the fuel assembly head. However, the spring protrudes from the fuel assembly head, for that reason the height of the holddown spring is higher than the one of the head.

In order to calculate the thermal expansion of the elements, the values of the thermal expansion coefficients are needed and taken from table 3.1.

With this data, an analytical and a numerical solution are compared in order to check whether the response of the model to temperature is similar to what it theoretically should be.

Thus, the thermal expansion of the fuel assembly at 300°C based on a reference temperature of 50°C has been calculated.

- Hot start-up at 300ºC.

Element	Thermal Expansion (mm)
Hold Down spring (Inconel X750)	7.7962 e-1
Head (SS304)	7.828 e-1
Guide Tubes (Zry-4)	6.1394
Foot (SS304)	7.828 e-1

Table 3.3 Theoretical thermal expansion of the fuel assembly elements at 300°C

- **ANSYS RESULTS.**

The gravity and the thermal loads are the only forces exerted in the structure during the simulation. Although the axial displacements due to the effect of gravity

are small in comparison to the axial displacements caused by thermal loads during operation, they cannot be neglected when analyzing the thermal expansion. For that reason, in order to achieve more accurate results, these displacements due to gravity are going to be taken into account.
Since the reference temperature is assumed to be 50ºC, the first simulation is done at this temperature, and the displacements due to gravity can be observed as the output (table 3.4).

- Simulation at 50ºC.

Node	Axial displacement due to gravity (mm)
15	-0.9915 e-1
14	-0.9915 e-1
13	-0.9915 e-1
2	-0.6336 e-3

Table 3.4 Analytical axial displacements due to gravity at 50°C

- Simulation hot start-up at 300ºC.

Node	Axial displacement (mm)	Axial displacement without the gravity effect (mm)
15	7.4966	7.5957
14	7.4693	7.5684
13	6.6939	6.7931
2	0.7747	0.7753

Table 3.5 Analytical axial displacements at 300°C

In table 3.5, the second column shows the output of the ANSYS simulation, and the third column shows these results minus the displacements from table 3.4.

These displacements result in the following analytical expansions of each element:

Element	Thermal Expansion (mm)
Hold Down spring (Inconel X750)	8.0260 e-1
Head (SS304)	7.7530 e-1
Guide Tubes (Zry-4)	6.0178
Foot (SS304)	7.7530 e-1

Table 3.6 Analytical thermal expansion at 300°C

- **COMPARISON OF ANALYTICAL AND EXPERIMENTAL RESULTS.**

Element	Analytical Thermal Expansion (mm)	Experimental Thermal Expansion (mm)	Deviation (%)
Hold Down spring (Inconel X750)	7.7962 e-1	8.0260 e-1	2.95
Head (SS304)	7.828 e-1	7.7530 e-1	0.96
Guide Tubes (Zry-4)	6.1394	6.0178	1.98
Foot (SS304)	7.828 e-1	7.7530 e-1	0.96

Table 3.7 Comparison of analytical and experimental results at 300°C

As the foregoing table shows, the deviations between the analytical and the experimental results are quite low which verifies the validity of the simulation. This means that the fuel assembly model responds correctly to the temperature changes.

3.5 Irradiation creep and growth

3.5.1 Irradiation creep on guide tubes and fuel rods

3.5.1.1 Introduction

Creep is a time dependent deformation of a material under the influence of mechanical stresses. This creep response of the material can occur as a result of long term exposure to high levels of stress, even if the stress is below the yield stress. Exposure temperature and time, applied load and material properties are factors that determine the magnitude of the deformation. Since these processes tend to soften the material they counteract the strain hardening produced by plastic deformation.

In mechanical responses to loading that are not time dependent such as elasticity and plasticity, the level of strain is set at the moment that the load is applied. On the contrary, in a time dependant process such as creep, the resulting strain is measured as a function of time.

Creep deformation in the nuclear reactor elements is considerably important during operation since the elements support axial stresses caused by all the axial forces that govern the reactor performance under hot condition. Moreover, this creep rate is enhanced by the neutron flux.

A commonly used equation for the representation of the creep model has the following form:

$$\dot{\varepsilon}_{creep} = A\,\sigma^{n}\,\phi^{p}\,exp\left(\frac{-Q}{RT}\right)\,t^{m} \qquad \textit{Equation 3.10}$$

Where:

A, n, m, p : Constants.

Q : Activation energy.

R: Gas constant.

T: Temperature.

ϕ: Fast neutron flux.

σ : Equivalent stress.

t : time

Two different models can be used to apply creep equations to variable in-reactor conditions: strain hardening and time hardening rules. These models are used to predict the creep curve under variable stress.

- Time hardening:

Time hardening anticipates that the change of the stress from a curve of stress σ_1 to a curve of stress σ_2 at t_1 will cause a change on the strain from the σ_1 curve to the σ_2 curve at t_1 , so that from t_1 to t_2 the curve continues at the σ_2 rate.
An example graph of time hardening is shown in the figure 3.14.

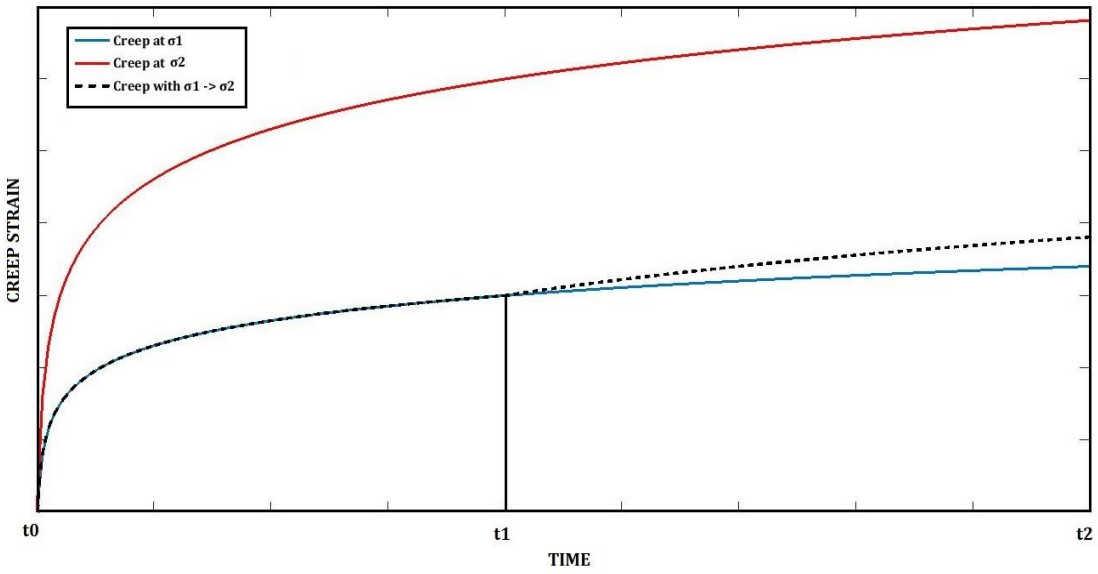

Figure 3.14 Schematic representation of time hardening.

However, zirconium alloys under pressure and thermal loads in nuclear reactors during operation seem to follow the strain hardening curve.

- Strain hardening:

In this case, strain hardening model predicts that the change of the stress from a curve of stress σ_1 to a curve of stress σ_2 will cause a change on the strain from the σ_1 curve to the σ_2 curve at ε_1 , so that the curve continues at the σ_2 rate from t_1 to t_2 .

Therefore, following this model, the creep strain rate depends on the stress and the accumulated strain.
An example representation of strain hardening is shown in figure 3.15.

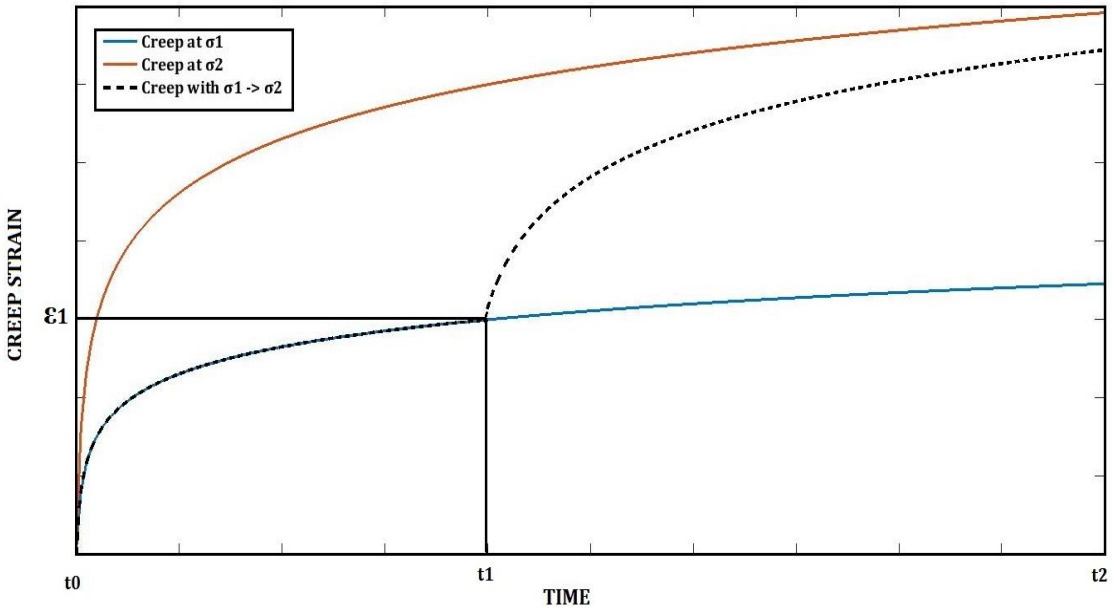

Figure 3.15 Schematic representation of strain hardening.

The relationship between these two models depends on the creep model. Thus, the total creep strain at the time of interest is:

$$\varepsilon_{cr} = A\,\sigma^{n}\,\phi^{p}\,\frac{t^{m+1}}{m+1}\exp\,(\frac{-Q}{RT}) \qquad \textit{Equation 3.11}$$

The creep rate equation is given by the derivate equation of the basic creep strain model (equation 3.11):

$$\dot{\varepsilon}_{cr} = A\,\sigma^{n}\,\phi^{p}\exp(\frac{-Q}{RT})\;t^{m} \qquad \textit{Equation 3.12}$$

Furthermore, from equation 3.11, the equivalent hardening time is obtained:

$$t_{hard} = \left[\frac{\varepsilon_{cr}\,(m+1)}{A\,\sigma^{n}\,\phi^{p}\exp\left(\frac{-Q}{RT}\right)}\right]^{\frac{1}{m+1}} \qquad \textit{Equation 3.13}$$

This hardening time (equation 3.13) can be introduced into the creep rate equation (equation 3.12), obtaining thus the strain hardening equation.

$$\dot{\varepsilon}_{cr} = \left[A\ \sigma^n\ \phi^p \exp(\frac{-Q}{RT})\ \varepsilon^m\ (m+1)^m\right]^{\frac{1}{m+1}} \qquad \textit{Equation 3.14}$$

This equation gives the creep rate as a function of the equivalent creep strain (ε).

3.5.1.2 Model description

In order to model the irradiation creep on guide tubes and fuel rods, the creep equations with their respective constants need to be implemented. These equations are characteristics of materials, and their constants are set using the following commands:

- **TB**, activates a data table for material properties or special element input.
  This command activates the "Creep" option, and the equation used to implement the creep.
  According to the two models that have been explained below, the Modified Time Hardening equation and the Modified Strain Equation can be selected by this command.

  - Modified Time Hardening:

$$\varepsilon_{cr} = \frac{C_1\ \sigma^{C_2}\ t^{C_3+1}\ e^{-C_4/T}}{C_3+1} \qquad \textit{Equation 3.15}$$

  - Modified Strain Hardening:

$$\dot{\varepsilon}_{cr} = \{C_1\ \sigma^{C_2}\ [(C_3+1)\varepsilon_{cr}]^{C_3}\}^{\frac{1}{C_3+1}}\ e^{\frac{-C_4}{T}} \qquad \textit{Equation 3.16}$$

Where:

ε_{cr} = equivalent creep strain

$\dot{\varepsilon}_{cr}$ = change in equivalent creep strain with respect to time
σ = equivalent stress
T =temperature
C_1, C_2, C_3, C_4 = constants
t = time at end of substep
e = natural logarithm base

- **TBDATA**, defines the constants of the selected equation in TB command.

In both time and strain hardening equations, C_1, C_2, C_3, C_4 constants have to be defined. In this study, these constants have been assumed according to the creep law provided by Yvon (1998) [20].

Q/R = 4700 K
A = 1.5 e-24
n = 0.8

Hence, the constants values can be calculated by comparing equation 3.15 and 3.16 to equation 3.10.

- Modified Time Hardening:

$C_1 = A * \phi^n * n =$ 1.5 e-24 * (1.13 e14 * 3600)$^{0.8}$ * 0.8
C_2 = 1
$C_3 = n - 1$ = - 0.2
C_4 = 4700

- Modified Strain Hardening:

$C_1 = A * \phi^n * n$ = 1.5 e-24 * (1.13 e14 * 3600)$^{0.8}$ * 0.8
C_2 = 1
C_3 = - 0.2
C_4 = 4700 * 1.25

Assuming thus the fast neutron flux within the reactor core:
ϕ = 1.13 e14 neutron/cm^{2}s

3.5.2 Irradiation growth on guide tubes and fuel rods

3.5.2.1 Introduction

While the presence of the irradiation creep needs the material to be under load, irradiation growth occurs without stress in the material. However, they both depend on similar microscopic processes in the material.

Neutron bombardment causes a high number of vacancies and interstitials within reactor environments. The accumulation of the so-called sinks in the material structure, attract other defects where they recombine and become trapped. If no stresses are applied, dislocations present in the lattice preferentially absorb the defects, causing them to climb. This phenomenon is known as irradiation growth.

The irradiation growth is a volume conservative distortion, only observed in non-cubic material structures. It is dependent on cold-work, so that cold-work materials normally grow more. It is also fluence and temperature dependent.

Thus, because the irradiation growth causes an axial length increase in the zircaloy-4 elements such as guide tubes and fuel rods, this process is relevant for the axial analysis of the fuel assembly.

3.5.2.2 Model description

The irradiation growth is modelled with the swelling option of ANSYS. Swelling is a material enlargement (volume expansion) caused by neutron bombardment or other effects (such as moisture). The swelling strain rate is generally nonlinear and is a function of factors such as temperature, time, neutron flux level, stress and moisture content. Irradiation induced swelling and creep is applied to metal alloys that are exposed to nuclear radiation.

This swelling option is implemented as a material property of the Zircaloy-4 with the TB and TBDATA commands. As a simplification, a linear swelling in guide tubes and fuel rods is selected, and these values are assumed:

- Fast neutron flux:

$$\phi = 1.13 \text{ e}14 \text{ neutron/cm}^2 \text{ s}$$

- Swelling constants:

- The swelling constant of the fuel rods is derived based on Nakano's experimental solution of the Zircaloy-4 fuel rod growth under fast neutron fluence.

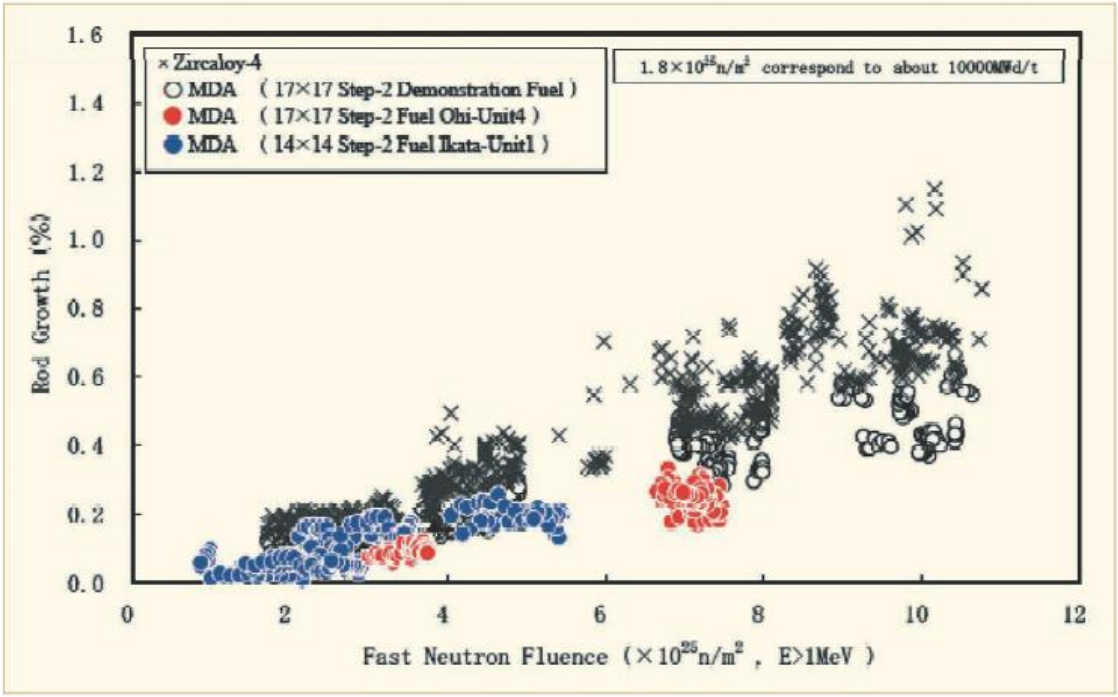

Figure 3.16 Graph- Nakano irradiation growth [21]

From figure 3.16, the following constant is derived by a linear regression:
$C_{Fuel\ Rod}$ = 0.767 e-16

- The swelling constant of the guide tubes is derived based on Garzarolli experimental solution of the irradiation growth. A linear regression of the fully recrystallized curve gives an approximate value for the swelling constant:

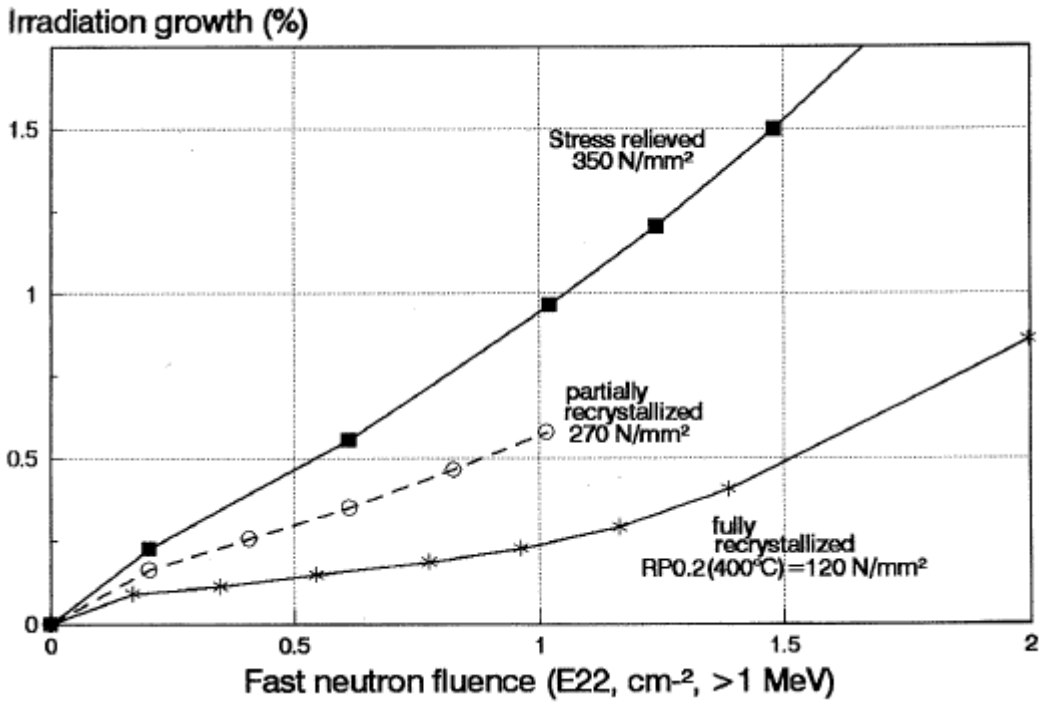

Figure 3.17 Graph- Garzarolli irradiation growth [18].

$C_{Guide\ Tube}$ = 0.4 e-16

Fuel tubes are cold-worked and normally grow more than guide tubes which are recrystallization annealed, for that reason the swelling constant of the fuel rods is nearly twice the constant of the guide tubes.

4. Results

The analysis of a complete fuel assembly irradiation cycle is performed in two sections. The first one is carried out over the initial start-up of the PWR operating cycle and the second one is performed over the irradiation cycle.

4.1 Analysis over the initial start-up of the PWR operating cycle

This section includes an analysis of the axial behavior of the fuel assembly during the first steps of the operating cycle (steps from 1 to 4, see section 1.5). The axial forces corresponding to these steps are applied progressively to the fuel assembly.

The evolution of the holddown force can be observed in figure 4.1, where five important points are highlighted (1-5).

The application of the holddown force is implemented progressively in 20 steps in the simulation. From step 0 to step 20 (see point 1 in figure 4.1), the evolution of the holddown force corresponds to the analysis done in section 4.2.4 (see figure 3.11).

Once the holddown force is applied and the structure is compressed, the transition from 50°C to 300°C (hot conditions) is implemented (see point 2). With the increase in temperature, the thermal expansion becomes relevant in the axial analysis. Thus, the core barrel, which is made of SS304, expands considerably more than the fuel assembly itself. Therefore, the core barrel thermal expansion results in a significant decrement of the holddown force. However, this decrement is partly counteracted by the thermal expansion of the fuel assembly, which increases the holddown force.

In the next step, the buoyancy forces are applied (see point 3). As expected, the buoyancy forces do not affect to the holddown force value.

Point 4 in the figure includes another change in the core temperature. In this step the temperature profile corresponding to nominal conditions is implemented (see figure 3.13). This temperature curve considers higher temperatures for fuel rods

than for guide tubes, and therefore the fuel rods suffer a higher thermal expansion than the guide tubes, setting the guide tubes under tensile stress. As a result, the holddown force slightly increases.

The last step of this analysis (see point 5) includes the effect of the hydrodynamic forces. As well as with the buoyancy forces, these forces do not affect to the holddown force value.

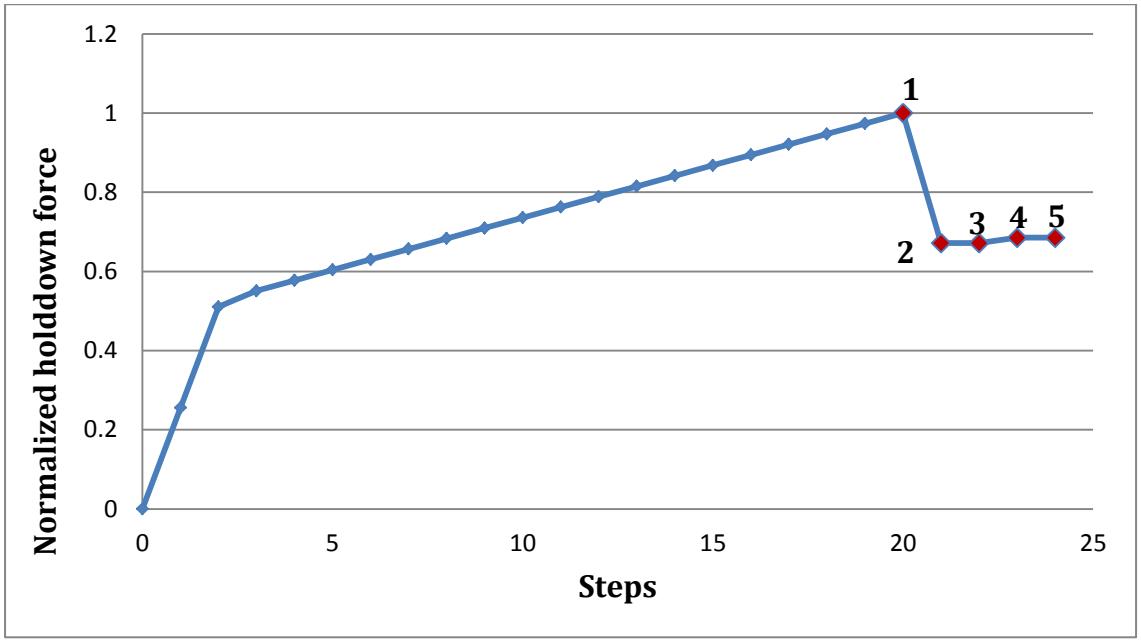

Figure 4.1 Graph- Simulated holddown force evolution during the first steps of the operating cycle

Figure 4.2 and figure 4.3 show, respectively, the progress of the axial stress on the fuel rods and guide tubes according to the steps studied on the holddown force evolution (see figure 4.1.). Once the holddown force is applied to the fuel assembly in the 20 first steps (see point 1), both guide tubes and fuel rods are compressed. When the PWR core is heated up from 50°C to 300°C (hot conditions) the compressive stress of these elements decreases slightly due to the effect of thermal expansion (see point 2). The effect of buoyancy forces on the next step (point 3) hardly affects the evolution of the axial stress in both guide thimbles and fuel rods. The most important alteration in the axial stress profile of these elements is caused by the temperature increase inside the PWR core according to the temperature curve in figure 3.13. This temperature profile corresponds to nominal conditions, and therefore, due to the fission events within the fuel rods, the temperature of the fuel rods is higher than the one of the guide tubes.

Consequently, the thermal expansion of the fuel rods is larger than the one of the guide thimbles.
As a result, at this point (see point 4) a significant change is produced in the axial stress evolution of both elements. Hence, the fuel rods become more compressed and the guide tubes move from a compressive axial stress to a tensile axial stress.
The last step (see point 5) includes the hydrodynamic forces of the coolant flow. These forces hardly affect to the axial stress of guide tubes and fuel rods.

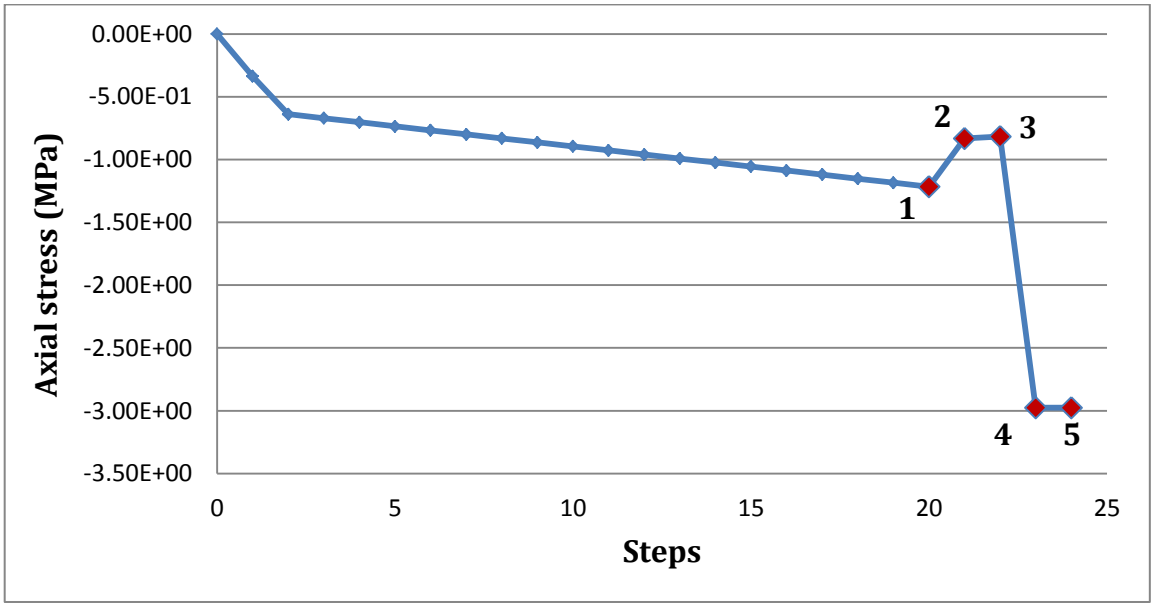

Figure 4.2 Graph- Simulated axial stress evolution of fuel rods during the first steps of the operating cycle

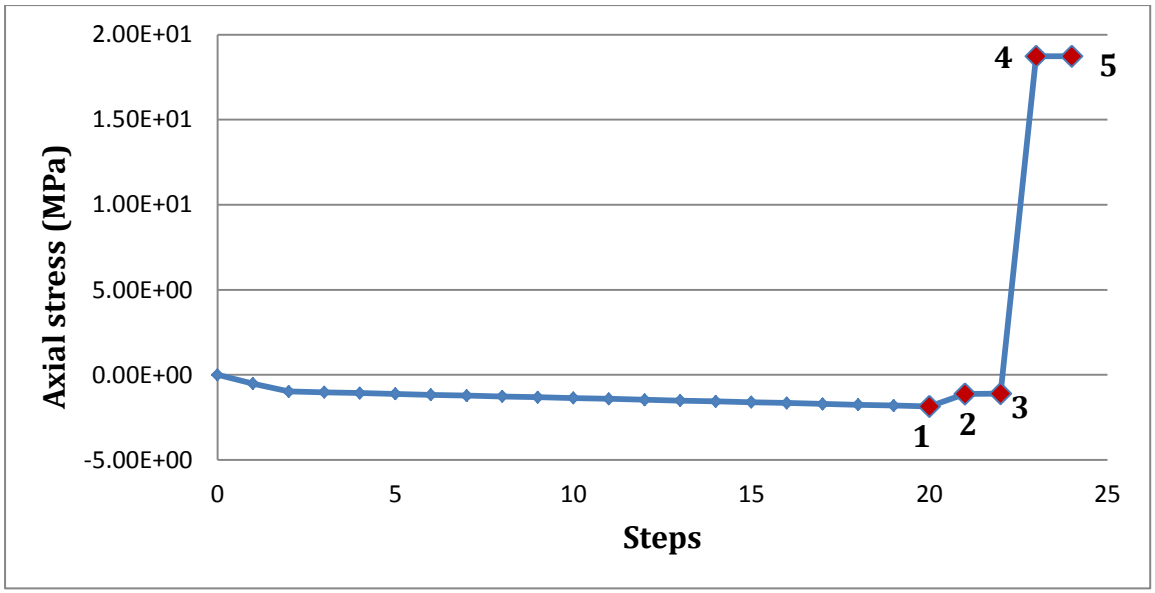

Figure 4.3 Graph- Simulated axial stress evolution of guide tubes during the first steps of the operating cycle

4.2 Analysis over the irradiation cycle

This section consists of a long term axial analysis of the fuel assembly during its irradiation phase. The first step assumed in this analysis is the last step of the analysis over the initial start-up of the PWR operating cycle in section 4.1.

The neutron flux within a PWR environment enhances irradiation creep and growth processes. These processes are time dependent with a large time scale, and, for that reason, this analysis is suitable over a large time interval.

These two types of deformation are the main cause of stress changes in the axial analysis of the fuel assembly during the irradiation stage.

4.2.1 Creep analysis

- Creep strain in guide tubes and fuel rods.

Figure 4.4 and figure 4.6 show the creep strain progress of both guide tubes and fuel rods, respectively, over time. In this analysis, the strain hardening model is selected since zirconium alloys under load seem to follow this model. Moreover, figure 4.5 and figure 4.7 illustrate the axial stress evolution of guide tubes and fuel rods over time.

The axial stress is initially positive in guide tubes since they are under tensile stress (see figure 4.5) and, as a result, the creep strain starts to increase with the time. This is because, under constant axial stress, the elements elongate plastically due to irradiation creep effect.
At the time the guide tubes elongate, the tensile stress in these elements decreases (relaxation of the elements). The relaxation of both guide tubes and fuel rods tend toward equilibrium between the axial stresses of these elements. Thus, the guide tubes, that are initially under tensile stress, become compressed at a certain point of the cycle (see point 1 in figure 4.5).

When the axial stress in guide tubes becomes negative, the creep strain in these elements begins to decrease (see point 1 in figure 4.4): the deformation of the guide tubes is negative in response to the compression which they are submitted to.

As figure 4.7 shows, the axial stress in fuel rods is initially negative, since they are compressed due to the temperature difference between guide thimbles and fuel rods. The compression of these elements causes the decrement of the creep strain over time, and, since the axial stress is negative throughout the whole cycle, the creep strain just decreases and never increases.

In both guide tubes and fuel rods, the relaxation of the axial stress can be observed. This relaxation is a consequence of the creep effect: the elements plastically elongate in response to the stress that is applied to them, and this elongation leads to a decrement of the axial stress.

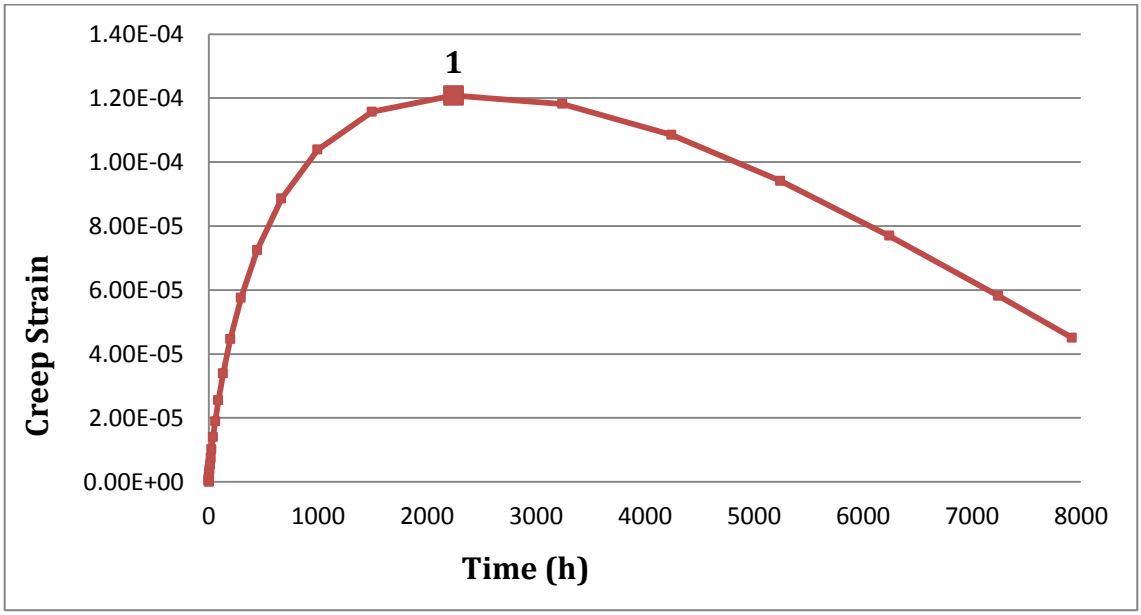

Figure 4.4 Graph- Simulated creep strain evolution of guide tubes over the irradiation stage

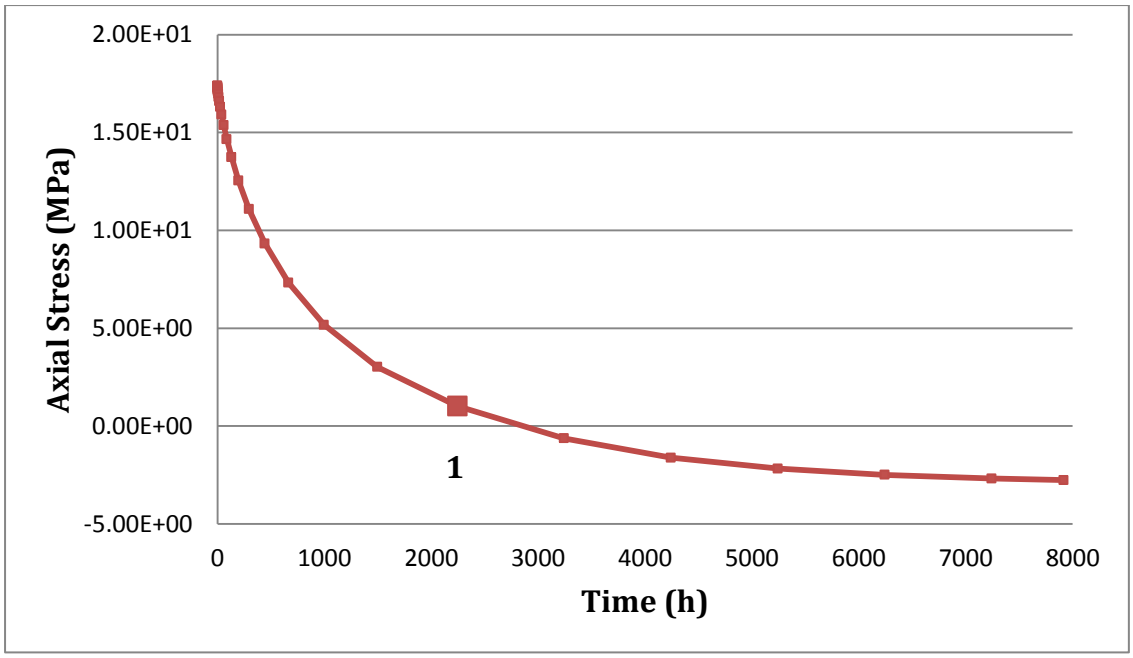

Figure 4.5 Graph- Simulated axial stress evolution of guide tubes over the irradiation stage

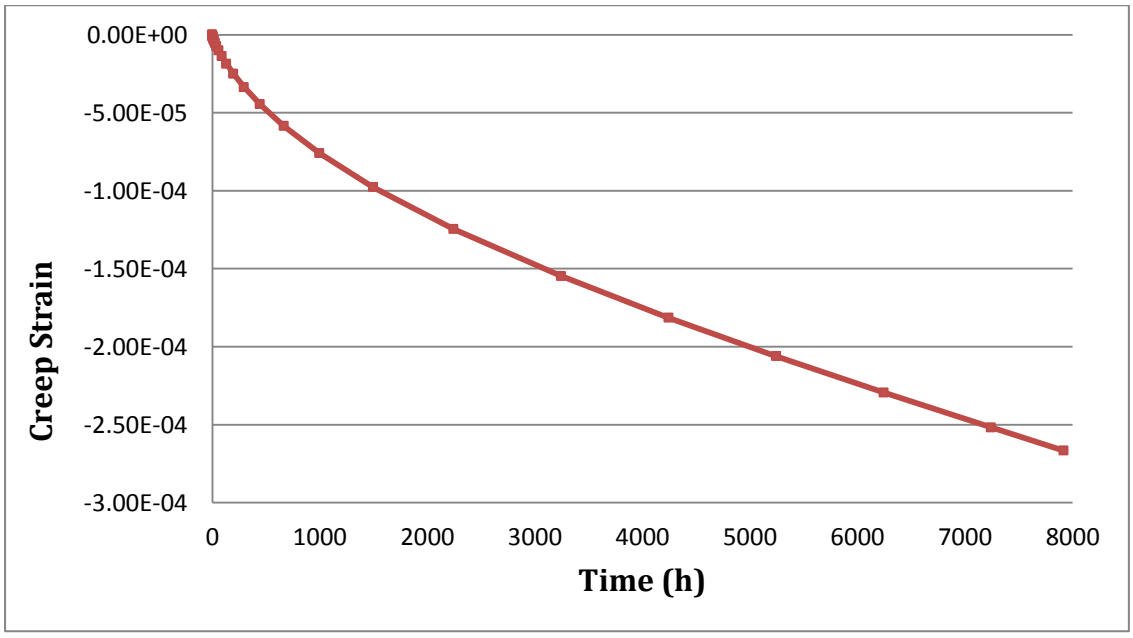

Figure 4.6 Graph- Simulated creep strain evolution of fuel rods over the irradiation stage

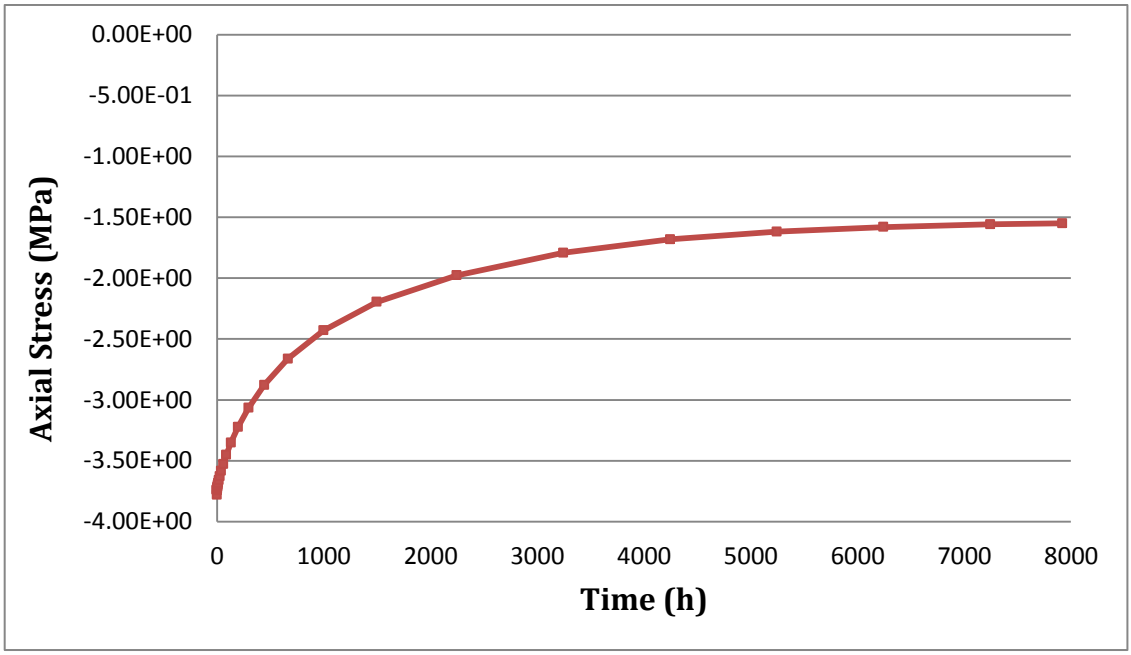

Figure 4.7 Graph- Simulated axial stress evolution of fuel rods over the irradiation stage

It is important to note that in this analysis, the relaxation of the springs in grid-to-rod connection has not been taken into account, and for this reason, the effect of the irradiation creep is considerably significant.

- <u>Comparison of creep effect with two different temperature profiles in fuel rods.</u>

  Figure 4.8 illustrates a comparison between two different temperature profiles of the fuel rods (see section 3.4.3). It shows the axial stress of both guide tubes and fuel rods as a function of time. Profile 1 considers lower temperatures of the fuel rods under irradiation, whereas profile 2 contemplates higher temperatures. Thus, higher temperatures in fuel rods do not only cause slightly larger compressive stress in these elements, but also considerably larger tensile stress in guide tubes. Moreover, the relaxation of guide tubes and fuel rods due to creep tend to equal the axial stresses value of these components (see profile 1). However, a larger temperature difference between fuel rods and guide tubes (see profile 2), leads to higher axial stresses in these elements, causing thus higher creep strains and therefore a larger relaxation of the tubes. As a result, the difference between the axial stresses of fuel rods and guide tubes at the end of the operating cycle is larger at higher temperatures at fuel rods (profile 2) than at lower temperatures (profile 1).

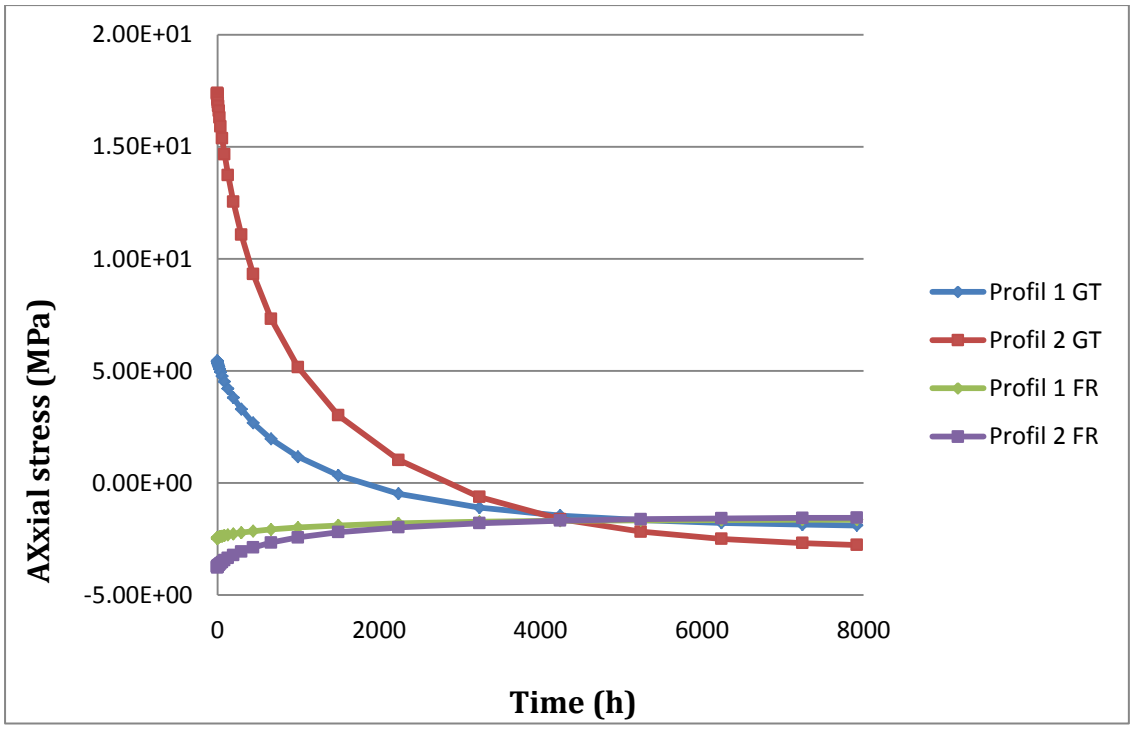

Figure 4.8 Graph- Simulated axial stress evolution of guide tubes and fuel rods for 2 temperature profiles

- <u>Creep analysis of guide tubes and fuel rods in different spans.</u>

  Figure 4.9 and figure 4.10 show the evolution of the axial stress in both guide tubes and fuel rods, respectively, over the PWR irradiation cycle (irradiation growth is not taken into account in this analysis). In both graphs all the guide tubes spans (regions subdivided by the grid levels) are shown, starting from the lowest span 1 (between foot and 1st grid) to the highest span 10 (between last grid and head).

  Regarding the guide tubes analysis (figure 4.9), all the intermediate spans follow the already explained pattern (see figure 4.5) since they are under tensile stress at the beginning of the cycle due to the effect of thermal expansion, and they finally become compressed at the end of the cycle due to the creep effect. However, the highest and lowest spans do not follow this behavior. Level 1 (lowest one) is compressed during the whole cycle due to the fact that the holddown force compresses the fuel assembly against the lower core plate, and therefore the lowest span of guide tubes support a higher compressive force that cannot be counteracted by the thermal expansion. Moreover, this level also supports the weight of the whole fuel assembly. Level 10 (highest one) is also under compressive stress during the entire operating cycle since the holddown force is

directly applied to the highest part of the fuel assembly. The relaxation of these guide tubes in comparison to the rest spans is negligible.

In the fuel rods axial analysis (see figure 4.10), the intermediate spans also follow the already explained curve (see figure 4.7). However, highest and lowest levels (1 and 10) are free ends of the fuel rods and, therefore, do not absorb any forces. Additionally, levels 2 and 9 show lower stress since the transmission of the reactive forces on the fuel rods is mainly distributed over the two uppermost and two lowermost grids. Hence, only intermediate levels (from 3 to 8) are entirely loaded.

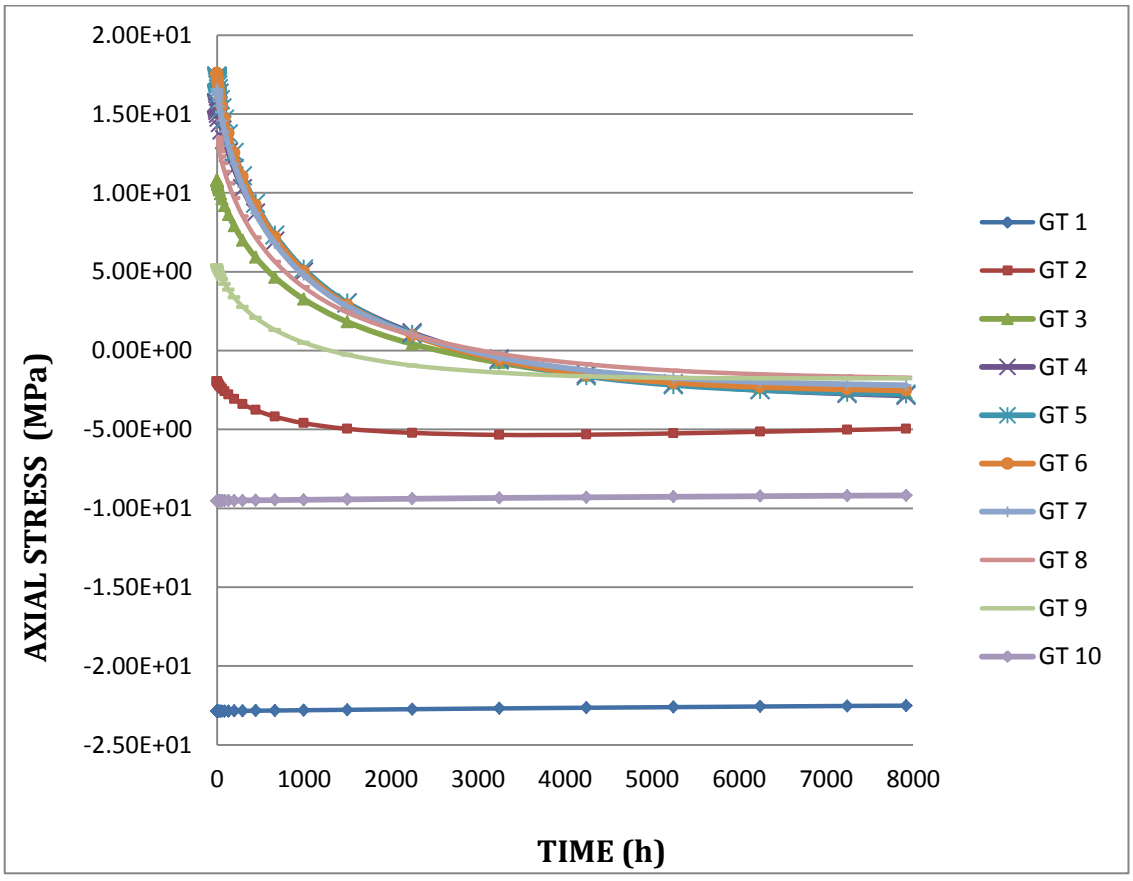

Figure 4.9 Graph- Simulated axial stress evolution of guide tubes in spans over the irradiation stage

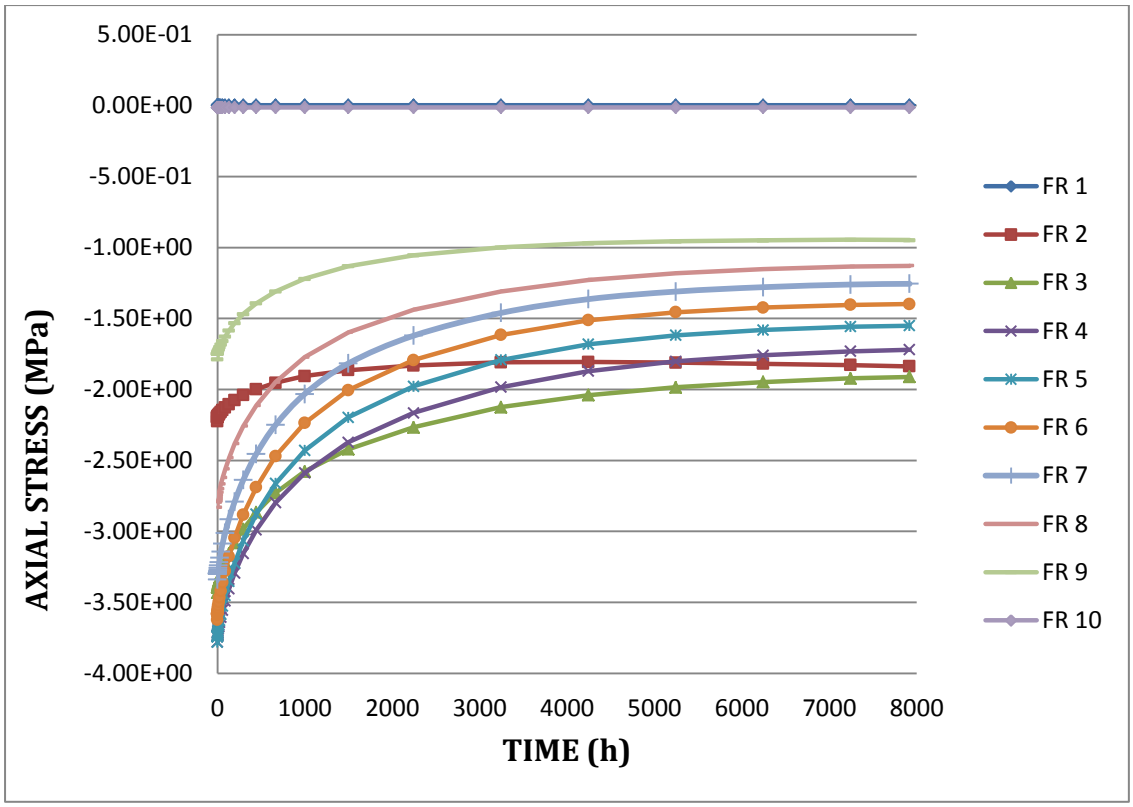

Figure 4.10 Graph- Simulated axial stress evolution of fuel rods in spans over the irradiation phase

4.2.2 Irradiation growth analysis

The guide tubes are under tensile stress at the beginning of the cycle, and this tensile stress decreases exponentially only if the irradiation creep effect is taken into account (see red line on figure 4.11). Thus, the guide tubes are initially under tensile stress and, at the end of the operating cycle, they become compressed as a response to the creep deformation.

Nevertheless, when the irradiation growth is included in the analysis, the axial stress of the guide tubes at the end of the cycle is still tensile (see green line on figure 4.11). This can be explained by the fact that the fuel rods tend to elongate more than guide tubes due to irradiation growth, since fuel rods are cold-worked (see section 3.5.2.2).

This elongation difference between guide tubes and fuel rods causes the fuel rods to become more compressed, whereas the guide tubes are under tensile stress.

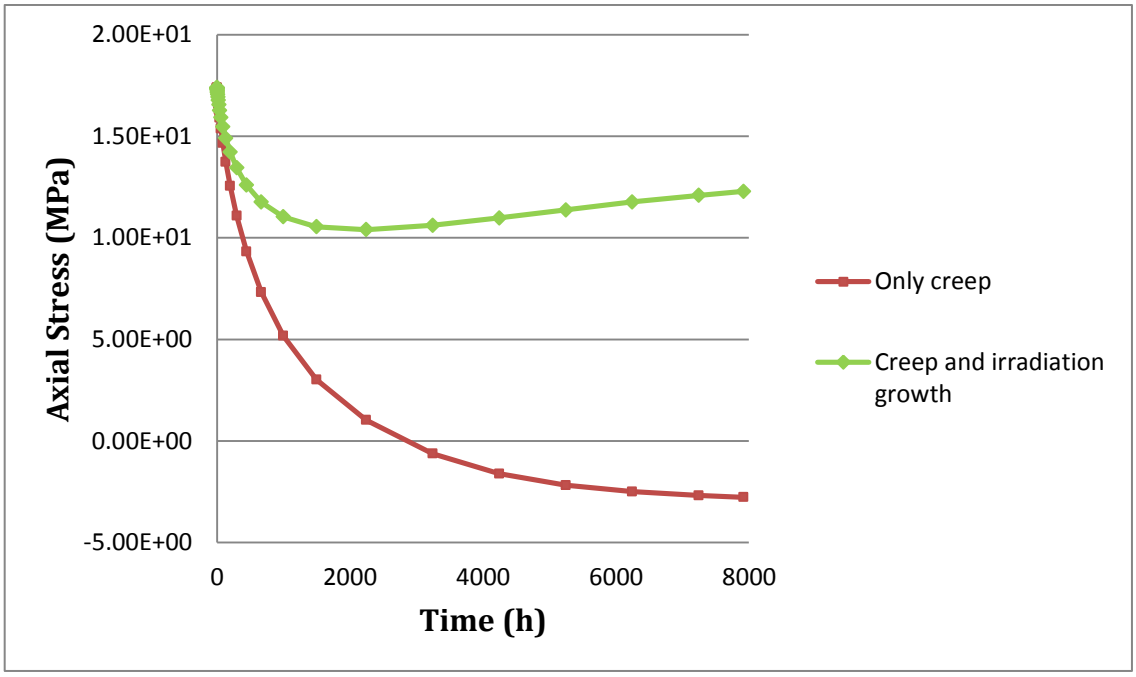

Figure 4.11Graph- Simulated axial stress evolution of guide tubes without irradiation growth vs. with irradiation growth effect

The guide tubes are under tensile stress at the beginning of the cycle, and this tensile stress decreases exponentially if only the irradiation creep effect is taken into account (see red line on figure 4.11). Thus, the guide tubes are initially under tensile stress and, at the end of the operating cycle, they become compressed as a response to the creep deformation.

Nevertheless, when the irradiation growth is included in the analysis, the axial stress of the guide tubes at the end of the cycle is still tensile (see green line on figure 4.11). This can be explained by the fact that the fuel rods tend to elongate more than guide tubes due to irradiation growth, since fuel rods are cold-worked (see section 3.5.2.2).

This elongation difference between guide tubes and fuel rods causes the fuel rods to become more compressed, whereas the guide tubes are under tensile stress.

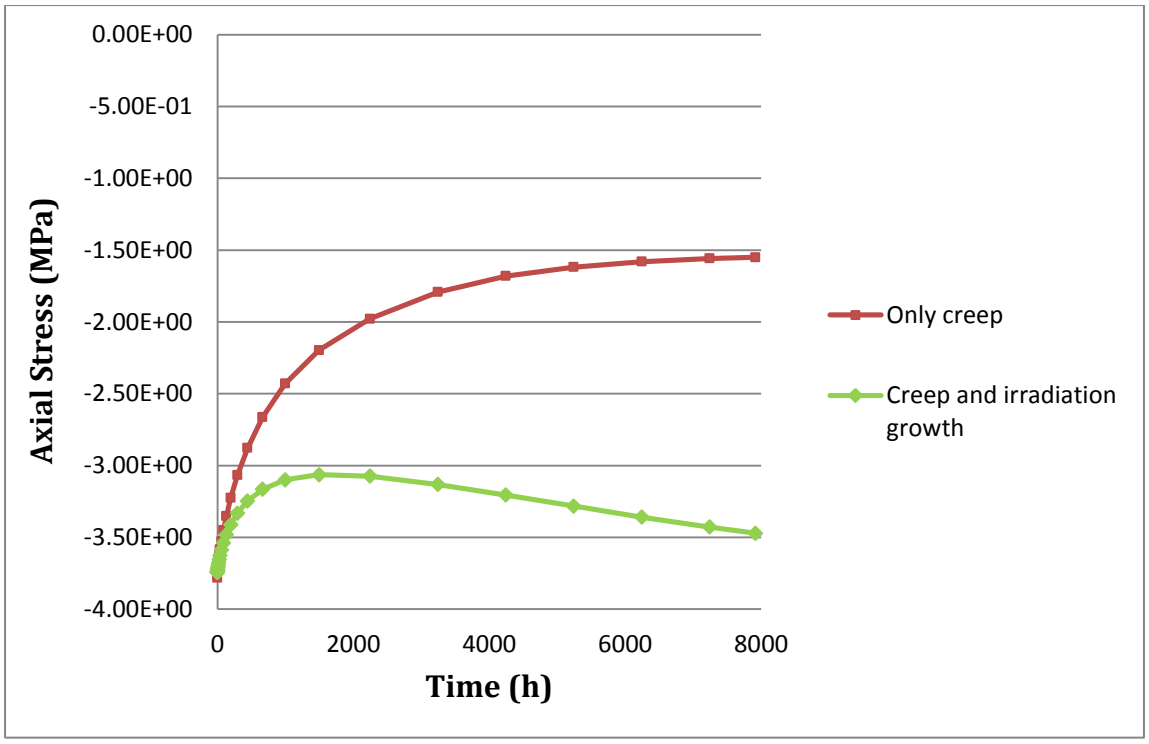

Figure 4.12 Graph- Simulated axial stress evolution of fuel rods without irradiation growth vs. with irradiation growth effect

The axial stress of the fuel rods is initially negative, and, without taking into account the effect of the irradiation growth, the compressive stress decreases exponentially due to irradiation creep (see red line in figure 4.12).

If the irradiation growth effect is included in the analysis, the compressive axial stress of fuel rods decreases at the beginning of the cycle due to the irradiation creep effect. However, the elongation of the tubes due to irradiation growth along the operating cycle causes an increment in the compressive stress (see green line in figure 4.12).

4.2.3 Holddown force analysis

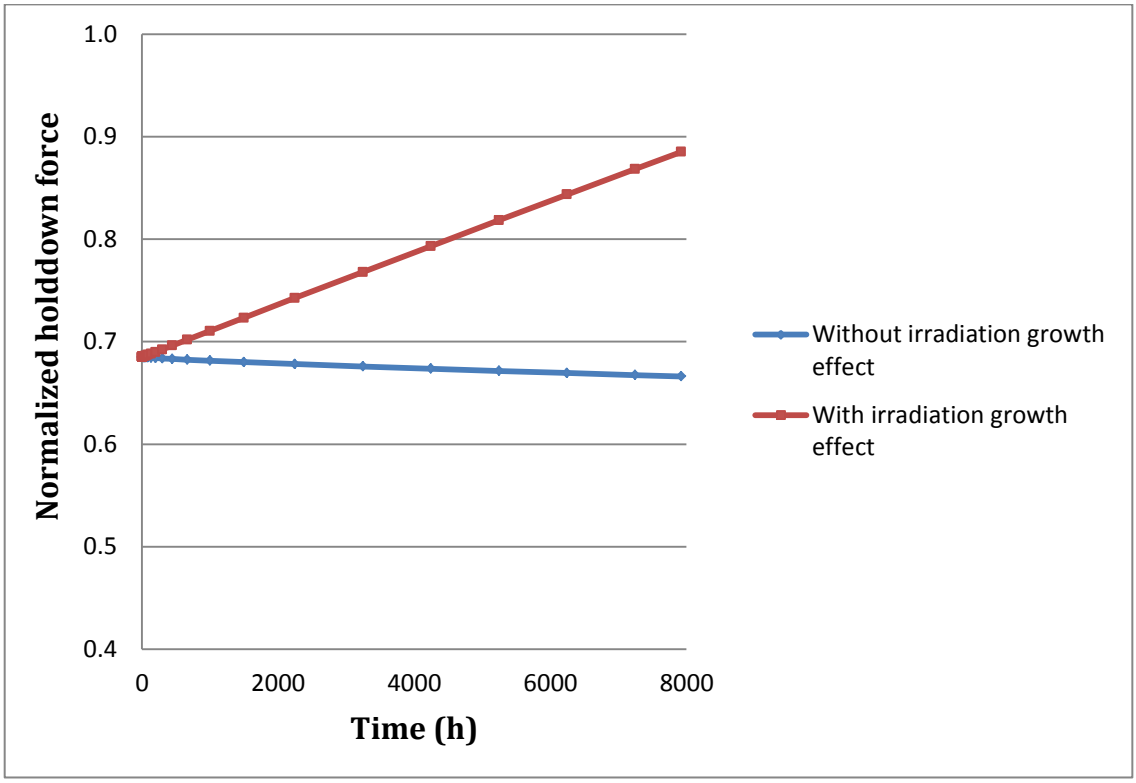

Figure 4.13 Graph- Simulated holddown force evolution over time without irradiation growth vs. with irradiation growth effect

The holddown force value is also affected by the changes in the fuel assembly height due to irradiation creep and growth. The starting holddown force value in figure 4.13 is the corresponding value of point 5 in figure 4.1.

The holddown force slightly decreases due to the irradiation creep effect. This can be explained by the relaxation of the elements due to creep. Thus, the guide tubes, which are initially under tensile stress, become compressed. This compression of the guide tubes causes a decrement on the holddown force (see red line in figure 4.13).

If the irradiation growth is taken into account, the tensile stress of guide tubes causes an increment in the holddown force throughout the irradiation cycle (see blue line in figure 4.13).

5. Conclusions and outlook

The objective of this Master´s Thesis was to perform a structural analysis of the irradiation-induced longitudinal growth of a PWR fuel assembly, as a part of the bow analysis of the fuel assemblies. This analysis is based on an existing finite element model of a typical PWR fuel assembly that has been implemented using ANSYS APDL simulation software.

At the beginning of the reactor start-up, the upper core plate is placed on the top of the fuel assembly so that the holddown springs compress the structure of the fuel assembly. Thus, the fuel assembly is prevented from lifting up due to the effect of the buoyancy and hydrodynamic forces, while absorbing the height change of the fuel assembly caused by thermal expansion. The hydrodynamic and buoyancy forces as well as the thermal expansion have an effect on the stresses of the fuel assembly structure and also on the holddown force. These effects are immediately observed and will be present during the complete operating cycle. However, both the force in the holddown spring and the stresses on the fuel assembly will be influenced by the irradiation creep and growth processes. Since these processes are time dependent in a large scale, the impact of irradiation creep and growth will only be significant over the entire irradiation cycle. For that reason, in order to achieve a more accurate knowledge of the structural axial changes of the fuel assembly, the simulation has been carried out in two parts. The first simulation has been performed for the initial start-up of the PWR operating cycle and the second one over the entire irradiation cycle.

The first study results show that the ANSYS model properly reproduces the temperature changes that occur on the fuel assemblies during the operation cycle. By applying the hot start-up temperature gradient to the entire fuel assembly structure, the thermal expansion truly meet the analytical values. Furthermore, as it was expected, when the nominal temperature curve was implemented, the fuel rods are compressed while the guide tubes are under tensile stress.

Regarding the simulation of the holddown force, the holddown spring was modeled by the COMBIN39 element. The results of the holddown force evolution in both studies demonstrate that the behavior of this element actually properly reproduces the physical behavior of the holddown device in a simplified way. As it is expected the value of the holddown force does not change when both the buoyancy and hydrodynamic forces are applied, since the purpose of the holddown force is to counteract these upward forces. However, the holddown

force responds as it is expected to changes on the fuel assembly height due to thermal expansion and irradiation creep and growth.

The results of the second study, which was carried out over the entire irradiation cycle, show that both creep and growth processes have an impact on the evolution of the axial stresses of the fuel assembly elements. As it was expected, irradiation creep leads to guide tubes and fuel rods stress relaxation. Figure 4.9 and Figure 4.10; meet a good agreement with the results of similar studies. Moreover, adding the effect of the irradiation growth, the effect of the irradiation creep becomes less significant. Furthermore, due to the fact that the irradiation growth effect is considerably higher in fuel rods than in guide tubes, the difference between fuel rods and guide tubes stresses increases at the end of the irradiation cycle when compared to the case where only irradiation creep is present.

In conclusion, since the model results show good agreement with the expected ones, it is proved that created the FEM ANSYS model provides a reliable basis for the study of the axial forces of a PWR fuel assembly.

However, in order to perform a complete bow analysis of a PWR FA, not only an axial analysis but also a lateral bow analysis is needed to be performed. For that reason, the implementation of the lateral bow forces in the complete FA model is proposed. Lateral forces within the in-reactor environment include structural loads (inter-assembly contact) and hydraulic loads (cross-flow). In addition, the relaxation of the springs in the grid-to-rod connection has not been taken into account in this analysis. The effect of the relaxation of these support springs decreases the effect of the irradiation creep and growth in guide tubes and fuel rods axial stresses over the operating cycle. Consequently, the implementation of the structural analysis of the irradiation-induced behavior of the fuel rod support in the complete model is also proposed for future works.

Acknowledgments

This thesis would not have been possible to write without the help and support of many people around me.

Firstly, I would like to thank Prof. Dr. Macián-Juan for bringing me the opportunity to write my Master's Thesis in the Department of Nuclear Engineering and for his continuous support. I would also like to express my deepest gratitude to Dipl. Ing. Andreas Wanninger for the guidance provided during the course of my work, his good advice and constant encouragement. I wish them all the best in their future.

I would also like to thank all the members of the department, for making my time here very pleasant, but especially to Dipl. –Ing. Jamel Rhouma for always showing his care for my work and personal motivation.

I want to thank my family, for all their support despite being far away.

I also thank all my friends with whom I have shared this wonderful experience in Munich. But especially, I would like to thank my "PC-Raum-Team" for making these six months unforgettable.

Special thanks indeed also to Greg O´Donnell for reviewing this work.

Finalmente, quisiera agradecer a mi abuelo Pepín, que me ha enseñado la importancia del esfuerzo, la constancia y el trabajo bien hecho para alcanzar grandes metas.

Bibliography

[1] Tomari-3 912 MW Nuclear Plant, J. (n.d). Power-technology.com. Retrieved April 2015, from *http://www.power-technology.com/projects/tomari-3/tomari-33.html*

[2] Macián, (2014), TU Munich, Course: Fundamentals of Nuclear Engineering, Lecture 1.

[3] U.S.NRC (March 2012). Retrieved April 2015, from *http://www.nrc.gov/reading-rm/basic-ref/teachers/reactor-fuel-assembly.html*

[4] Yu Wenchi, G.Y. (2011). PWR Fuel element stability analysis. Shenzhen, China.

[5] Peter Rundling, T.I. (2004). PWR Fuel Failure Management Handbook. Surahammar, Sweden.

[6] Wanninger, A. (2015, January 16). Development of Computational Methods to Describe the In-Reactor Mechanical Behavior of PWR Fuel Assemblies. Garching, Bayern, Germany.

[7] ANSYS Mechanical APDL Element Reference. (2012). ANSYS, Inc.

[8] ANSYS Mechanical APDL Material Reference. (2012). ANSYS, Inc.

[9] ANSYS Mechanical APDL Command Reference. (2012). ANSYS, Inc.

[10] Operating Principles of Nuclear Power Plants. FEMA Emergency Management Institute. Retrieved April 2015, from *http://emilms.fema.gov/IS3/FEMA_IS/is03/REM0402180.htm*

[11] Fuel Assemblies in Nuclear Reactors. Justin Carr, Rick Wagner, Rich Vargo. Retrieved April 2015, from *http://me1065.wikidot.com/fuel-assemblies-in-nuclear-reactors*

[12] S.Y.Jeon, N.G.Park, G.T.Choi, H.K.Kim (2007). An investigation on the holddown margin using Monte-Carlo Algorithm for the PWR Fuel Assembly.

[13] Thermophysical properties database of materials for light water reactors and heavy water reactors. (June 2006). IAEA.

[14] Inconel alloy X-750. Special metals. Retrieved April 2015, from *www.specialsmetals.com*

[15] Product Data Sheet 304/304L Stainless Steel. AK Steel. *www.aksteel.com*

[16] Review of Zircaloy-2 and Zircaloy-4 properties relevant to N.S Savannah Reactor Design. C.L.Whitmarsh.

[17] B.Levasseur, G.Chaigne, R.Fernandes (2009). 3D Modeling of Fuel Assembly bow for EDF PWRs. Paris, France.

[18] G.Kessler,(2104) The Risk of Nuclear Energy Technology- Safety concepts of Light Water Reactors. Springer

[19] Fuel Design Data. Nuclear Engineering International (2004). Retrieved April 2015, from *http://www.docstoc.com/docs/146041434/Fuel-design-data---Nuclear-Engineering-International*

[20] P.Yvon, J.Diz, N.Ligneau (1998). Irradiation creep and growth of guide thimble alloys. French Nuclear Energy Society.

[21] Nakano T., Fujii H. and Shimizu J., "Mitsubishi PWR Fuel Experience and Reliability", Proceedings of 2008 Water Reactor Fuel Performance, Seoul, Korea, paper 8066, October, 2008.

[22] F.Garzarolli, H.Stehle, E.Steinberg (1996). Behavior and properties of Zircaloys in Power Reactors: A short review of pertinent aspects in LWR Fuel.

[23] S.Was, G. (2007). Fundamentals of Radiation Material Science- Metals and alloys. Springer.